
R-Stitch: Dynamic Trajectory Stitching for Efficient Reasoning

Zhuokun Chen¹ Zeren Chen² Jiahao He³ Lu Sheng² Mingkui Tan⁴ Jianfei Cai¹ Bohan Zhuang^{3†}

Abstract

Chain-of-thought (CoT) improves the reasoning ability of large language models (LLMs) but incurs substantial inference cost due to long autoregressive trajectories. Existing acceleration methods either shorten reasoning traces or rely on speculative decoding with a smaller model. However, speculative decoding offers limited speedup when model agreement is low and rigidly enforces token-level consistency, failing to exploit the fact that smaller models often produce much shorter reasoning traces when correct. We introduce *R-Stitch*, a training-free hybrid decoding framework that delegates token-level computation between a small language model (SLM) and an LLM using entropy as an uncertainty proxy. High-uncertainty tokens are routed to the LLM, while low-uncertainty tokens are handled by the SLM, avoiding full rollbacks and preserving answer quality. We further propose *R-Stitch*⁺, which learns an adaptive routing policy to dynamically adjust token budgets beyond fixed thresholds. By jointly reducing per-token decoding cost and the number of generated tokens, our approach achieves substantial acceleration with negligible accuracy loss. It attains peak speedups of $3.00\times$ on DeepSeek-R1-Distill-Qwen-7B, $3.85\times$ on 14B, and $4.10\times$ on QWQ-32B, while maintaining accuracy comparable to full LLM decoding. Moreover, R-Stitch enables flexible efficiency-accuracy trade-offs under diverse computational budgets without retraining. Project is available at <https://caesarhhh.github.io/R-Stitch>.

larly when combined with chain-of-thought (CoT) prompting (Wei et al., 2022; Zhang et al., 2024; Zheng et al., 2024). By generating intermediate reasoning steps token-by-token, CoT enables LLMs to solve complex problems in arithmetic, logic, and code generation (Wei et al., 2022; Kojima et al., 2022; Zhang et al., 2023). However, this autoregressive decoding process is inherently slow, as each token requires a full forward pass through the model (Liu et al., 2024; Sadhukhan et al., 2024; Chen et al., 2023). The latency becomes especially problematic in CoT, where outputs often span thousands of tokens, significantly limiting the applicability of LLMs in time-sensitive scenarios.

To address this bottleneck, recent efforts have primarily focused on three directions: reducing the number of generated tokens, applying speculative decoding to accelerate the generation process, and optimizing KV cache access during long-context decoding. The first direction includes approaches that aim to shorten CoT sequences, such as early exiting or incorporating length-aware reward functions during Reinforcement Learning (RL) (Fatemi et al., 2025; Yang et al., 2025b; Ma et al., 2025; Yi et al., 2025; Jiang et al., 2025). The second leverages a small language model (SLM) to draft multiple tokens ahead, which are then verified in parallel by a larger LLM (Liu et al., 2024; Sadhukhan et al., 2024; Chen et al., 2023). If verification succeeds, the drafts are accepted; otherwise, generation rolls back to the last matching token. The third direction addresses the I/O bottleneck introduced by repeated access to large key-value (KV) caches during decoding, which becomes increasingly expensive in long-context reasoning. Techniques such as sparse or selective KV caching (Gao et al., 2025; Tang et al., 2024) have been proposed to reduce memory traffic and improve decoding speed on modern hardware.

Among the three directions, speculative decoding has received considerable attention due to its potential for substantial speedups. However, its effectiveness critically depends on the consistency between the small language model (SLM) and the large language model (LLM). We quantify this limitation using token-level consistency, defined as the percentage of tokens for which the SLM produces the same output as the LLM given an identical prefix. Figure 1a presents token-level consistency and decoding speedup in speculative decoding across four model combinations on the AMC dataset: DeepSeek-R1-Distill-Qwen-1.5B/7B (Guo

1. Introduction

Large language models (LLMs) have achieved impressive performance on a wide range of reasoning tasks, particu-

¹Monash University, Australia ²School of Software, Beihang University, China ³ZIP Lab, Zhejiang University, China ⁴South China University of Technology, China. Correspondence to: Zhuokun Chen <caesard216@gmail.com>, Bohan Zhuang <bohan.zhuang@gmail.com>.

et al., 2025), L1-1.5B-Short (Aggarwal & Welleck, 2025) and Qwen2.5-Math-1.5B/7B-Oat-Zero (Liu et al., 2025). The results show a clear trend: lower consistency correlates with smaller speedup, particularly in reasoning-intensive tasks. Figure 1b shows the distribution of speedup ratios across individual samples from the AMC dataset, using DeepSeek-R1-Distill-Qwen-7B as the LLM and L1-Short as the SLM. While some samples achieve noticeable acceleration, a large number have speedups below $1\times$, indicating that speculative decoding can introduce overhead on certain inputs. Furthermore, Figure 1c compares the number of tokens generated by the same SLM and LLM on questions both models answer correctly. The SLM produces much shorter completions, suggesting that speculative decoding’s rigid reliance on exact token agreement may prevent it from utilizing the SLM’s more concise reasoning effectively.

To more flexibly exploit SLM for acceleration, we propose R-Stitch, an entropy-guided decoding framework inspired by the preceding observations. Our empirical analysis shows that tokens with higher entropy are more error-prone, which motivates a token-level routing strategy: the SLM acts as the primary generator, and the LLM is invoked only when needed. In this framework, confident low-entropy tokens are accepted directly from the SLM, while uncertain high-entropy tokens trigger LLM intervention for correction and continued generation. Compared with agreement-based speculative decoding, this dynamic delegation avoids full-sequence rollbacks, preserves the complementary strengths of both models, and achieves efficient reasoning under tight computational budgets.

To refine the entropy-based heuristic, we introduce R-Stitch⁺. Rather than relying on a fixed threshold, R-Stitch⁺ equips high-uncertainty tokens with a lightweight router that determines whether LLM intervention is necessary. The router is trained via RL with a latency-aware reward, enabling a data-driven policy that adaptively balances accuracy and efficiency. Thus, R-Stitch⁺ extends the heuristic rule of R-Stitch into a more effective routing mechanism under diverse conditions.

We validate our proposed method on five challenging mathematical reasoning benchmarks using DeepSeek-R1-Distill-Qwen models at 7B, 14B, and 32B scales. Across all settings, our approach achieves substantial latency reduction while maintaining accuracy close to full LLM decoding, reaching peak speedups of $3.00\times$, $3.85\times$, and $4.10\times$ on the 7B, 14B, and 32B models, respectively. Overall, these results confirm that token-level, entropy-guided collaboration provides a principled and effective solution for accelerating CoT reasoning, addressing the limitations of speculative decoding and enabling flexible deployment under different computational budgets.

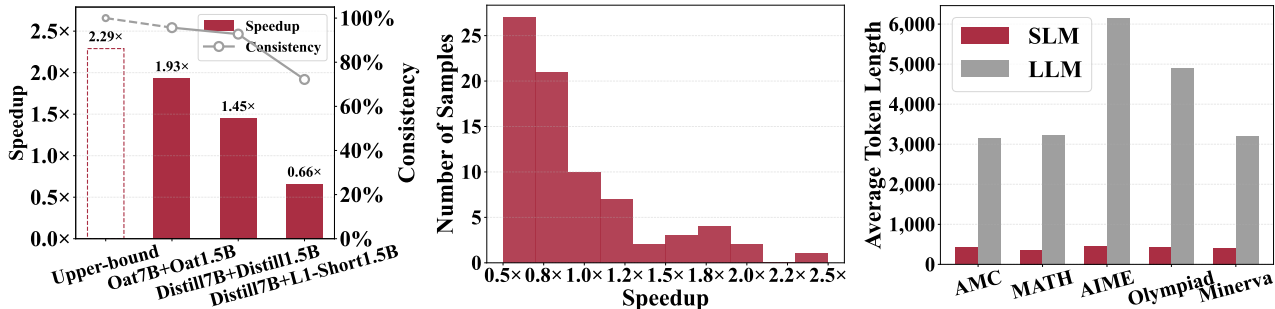
Our contributions are summarized as follows:

- We analyze the limitations of speculative decoding in low-consistency CoT settings and show that its rigid alignment with the LLM can sacrifice potential efficiency gains from the SLM.
- We analyze the entropy distribution of tokens in CoT reasoning and reveal its strong correlation with prediction errors, motivating entropy as an effective routing signal.
- We propose R-Stitch, an entropy-guided hybrid decoding paradigm that adaptively switches between the SLM and LLM to accelerate CoT generation without requiring additional training. We further extend it to R-Stitch⁺, which learns a routing policy with a latency-aware RL reward, enabling more optimal efficiency–accuracy trade-offs.
- Extensive experiments on mathematical reasoning benchmarks demonstrate that our method achieves consistently lower latency at the same level of accuracy compared with speculative decoding.

2. Related Work

LLM reasoning. Recent advances in prompting strategies have significantly improved the reasoning capabilities of LLMs, enabling them to solve complex tasks through structured intermediate computation. A variety of inference-time strategies have been proposed to enhance reasoning, primarily including Chain-of-Thought (CoT) (Wei et al., 2022; Zhang et al., 2024; Zheng et al., 2024), Tree-of-Thought (Yao et al., 2023), and Monte Carlo Tree Search (MCTS)-based decoding (Zhang et al.). Among these, CoT has emerged as a widely adopted method that guides the model to verbalize intermediate steps instead of directly predicting the final answer (Wei et al., 2022; Kojima et al., 2022; Zhang et al., 2023; Li et al., 2025a), improving performance on arithmetic and code reasoning benchmarks. However, these approaches often rely on token-by-token autoregressive decoding of long reasoning chains, which can be inefficient and lead to high inference latency, limiting their scalability in real-world applications.

Accelerating reasoning in LLMs. Improving the efficiency of chain-of-thought (CoT) reasoning involves addressing three key bottlenecks: reasoning length, per-token decoding cost, and KV cache I/O overhead. The first focuses on reducing the number of generated tokens by shortening reasoning chains. Methods such as Concise Reasoning (Fatemi et al., 2025) and ShorterBetter (Yi et al., 2025) use length-aware rewards to promote brevity without sacrificing correctness. Other approaches, including DEER (Yang et al., 2025b) and ThinkPrune (Hou et al., 2025), leverage model entropy or attention patterns to eliminate unnecessary steps, while



(a) Token-level consistency versus speedup across different LLMs. (b) Speedup across individual samples in AMC. (c) Token usage on questions answered correctly by SLM and LLM.

Figure 1. Token-level consistency and speedup analysis. (a) shows the relationship between token-level consistency and speedup in speculative decoding across different LLM-SLM pairs on AMC. (b) presents the distribution of speedup ratios across individual samples from AMC. (c) illustrates the token counts for questions correctly answered by both the SLM and LLM.

methods like AdaptThink (Zhang et al., 2025) and Think-Less (Fang et al., 2025) aim to skip reasoning entirely when it is not needed. These techniques effectively reduce sequence length, thereby lowering total decoding time. The second line of work targets per-token decoding complexity. Speculative decoding (Liu et al., 2024; Sadhukhan et al., 2024; Chen et al., 2023) speeds up generation by having a small language model (SLM) propose token drafts, which are verified in parallel by a large LLM. However, low agreement between the SLM and LLM often causes frequent rollbacks, limiting acceleration gains. Finally, recent research (Gao et al., 2025) (Tang et al., 2024) has highlighted the importance of reducing KV cache I/O—an increasingly dominant cost in long-context decoding, which also happens during the inference phase of reasoning models due to the length of CoT. Since decoding is often I/O-bound, reducing the loading of KV cache from global memory to on-chip memory of GPUs (e.g., via sparse or selective KV caching) can significantly improve system throughput.

Stitching. Stitching broadly refers to composing multiple models or modules into a unified inference process, often by connecting their intermediate representations or generation trajectories. Early approaches like SN-Net (Pan et al., 2023), SN-Net v2 (Pan et al., 2024), and ESTA (He et al., 2024b) focused on layer-wise stitching within single-modality models, enabling efficient adaptation across backbone variants. Other works such as T-Stitch (Pan et al., 2025b) extended stitching to the trajectory level, applying diffusion-based denoising to merge reasoning paths. Beyond single domains, cross-model stitching has also emerged—LLaVA (Liu et al., 2023), for example, connects a vision encoder with an LLM to build a multi-modal agent. More recent efforts explore general-purpose stitching frameworks, such as Meta-Query (Pan et al., 2025a) and UniWorld (Lin et al., 2025), which introduce connector modules (e.g., MLPs or learned queries) to link heterogeneous models. Our work follows this trend by stitching a small and large language model

at the token level during autoregressive decoding, enabling efficient collaboration without expensive retraining.

3. Methodology

In this section, we build on our empirical finding that high-entropy tokens are more likely to induce errors, and present R-Stitch, a collaborative decoding framework that uses entropy as an uncertainty proxy to coordinate the SLM and LLM. R-Stitch accepts SLM tokens when entropy is low to reduce latency, while delegating high-entropy tokens to the LLM for reliable decoding. This entropy-guided routing exploits the complementary strengths of heterogeneous models and underpins the RL extension R-Stitch⁺, which learns an adaptive policy beyond fixed thresholds.

3.1. Preliminary

Hybrid decoding setting. We study a hybrid inference setup with a SLM f_{SLM} and a LLM f_{LLM} , both autoregressive and sharing the same tokenizer. Given a prompt x , the model generates a token sequence $y_{1:T} = [y_1, y_2, \dots, y_T]$ in an autoregressive manner. At decoding step t , the active model $f \in \{f_{\text{SLM}}, f_{\text{LLM}}\}$ outputs a probability distribution $\mathbf{p}_t = f(y_{1:t-1})$, from which the next token y_t is sampled.

3.2. Bidirectional Entropy-Guided Decoding

3.2.1. EMPIRICAL ENTROPY ANALYSIS

LLMs exhibit stronger reasoning capabilities but incur substantially higher inference costs compared to SLMs. Prior work shows that when the two models produce consistent outputs, delegating computation to the SLM can effectively reduce latency. This raises a fundamental question: under what conditions can SLM predictions be relied upon without compromising correctness? To answer this, we conduct sample- and token-level entropy analyses on AMC using

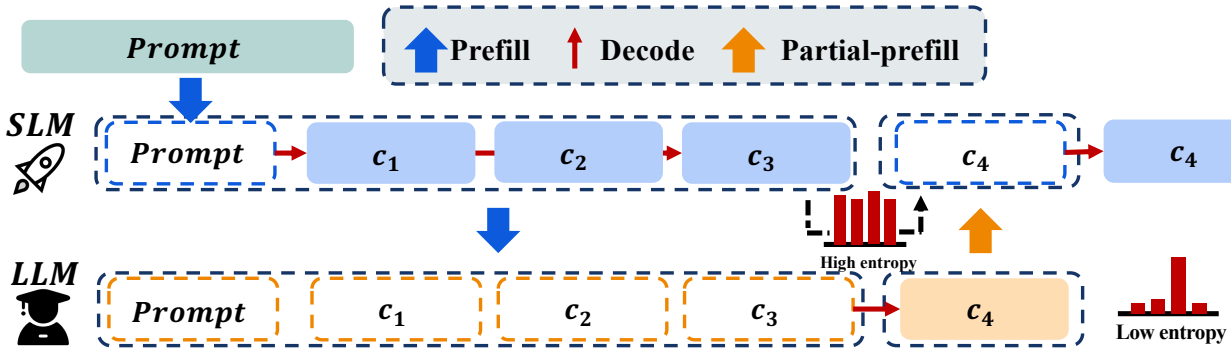


Figure 2. **Overview of R-Stitch.** Given a question with CoT prompting, decoding alternates between an SLM and an LLM under an entropy-based switching policy. Generation starts with the SLM; tokens with low entropy are accepted directly, while high-entropy tokens trigger the LLM to overwrite them and resume decoding. Symmetrically, when the LLM outputs a low-entropy token, it returns to the SLM to reduce computational cost. This bidirectional mechanism adaptively allocates computation, preserving SLM efficiency while leveraging LLM reliability when needed.

DeepSeek-R1-Distill-Qwen-7B (LLM) and L1-1.5B-Short (SLM), which reveal the following empirical patterns.

1. Elevated uncertainty is associated with error-prone regions. On AMC, the mean entropy over generated tokens is higher in incorrect reasoning traces than in correct ones (Figure 3a). To further localize this effect, we analyze *harmful tokens*, defined as the first SLM-generated tokens whose inclusion flips the LLM’s answer from correct to incorrect, restricting the analysis to cases where the LLM succeeds but the SLM fails. As shown in Figure 3c, the local context preceding such harmful tokens consistently exhibits higher entropy than the overall token distribution, indicating that errors tend to arise in locally uncertain regions.

2. Most tokens are generated with extremely low uncertainty. We analyze the entropy distribution across reasoning sequences. As shown in Figure 3b, the distribution is heavily skewed toward zero: only 10.65% of SLM-generated tokens exceed an entropy of 0.1, while the majority have entropy exactly 0. This shows that high-entropy tokens are relatively rare within a sequence.

3.2.2. METHOD

Building on these findings, we design R-Stitch to explicitly exploit the observed link between token entropy and error likelihood. R-Stitch is a token-level decoding framework that dynamically alternates between the SLM and LLM based on entropy-derived uncertainty. The key idea is to let the SLM decode as much as possible to reduce latency, while invoking the LLM only when necessary to maintain answer quality. Importantly, the LLM can also transfer control back to the SLM once low-entropy (high-certainty) tokens are reached, enabling a full bidirectional flow. We use a predefined threshold τ to balance the latency–accuracy trade-off.

Entropy-guided stitching. At each decoding step t , the active model produces a probability distribution \mathbf{p}_t over the vocabulary of size V . We quantify uncertainty by the normalized entropy of this distribution:

$$\mathcal{H}_t = \frac{-\sum_{i=1}^V p_{t,i} \log p_{t,i}}{\log V}, \quad \mathcal{H}_t \in [0, 1]. \quad (1)$$

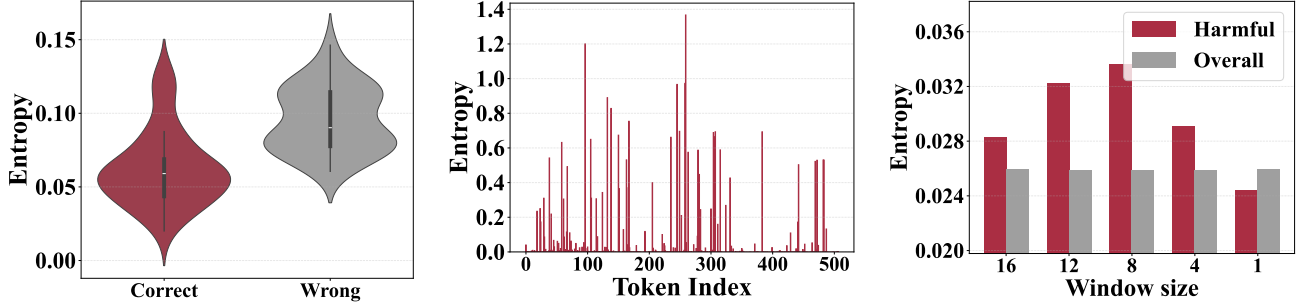
Larger \mathcal{H}_t indicates higher uncertainty, while smaller values indicate higher certainty.

Decoding begins with the SLM. At each step t , if the uncertainty $\mathcal{H}_t^{\text{SLM}} \leq \tau$, the SLM accepts its prediction and proceeds. Otherwise ($\mathcal{H}_t^{\text{SLM}} > \tau$), the token is discarded and the step is reprocessed by the LLM, which resumes decoding. Symmetrically, while decoding with the LLM, if $\mathcal{H}_t^{\text{LLM}} \leq \tau$, control is handed back to the SLM; otherwise, the LLM continues.

Formally, the switching policy is:

$$\text{Switch}(t) = \begin{cases} \text{SLM} \rightarrow \text{LLM} & \text{if } \mathcal{H}_t^{\text{SLM}} > \tau, \\ \text{LLM} \rightarrow \text{SLM} & \text{if } \mathcal{H}_t^{\text{LLM}} \leq \tau. \end{cases} \quad (2)$$

KV Cache management. R-Stitch maintains separate key-value caches for the SLM and LLM. When a model first participates in reasoning, it performs a full prefill over the existing input context to initialize its KV cache. Thereafter, each model incrementally updates its own cache during decoding. During model switches, we avoid redundant computation by leveraging *partial prefill*. Specifically, when switching back to a model that has previously decoded, we reuse its existing KV cache and only prefill the new tokens generated by the other model since the last switch. This strategy eliminates repeated attention over already-processed tokens, thereby enabling efficient cache reuse and significantly reducing switching overhead.



(a) Sample-level entropy in correct vs. incorrect solutions

(b) Token-level entropy distribution across full reasoning traces

(c) Elevated entropy around the first harmful token

Figure 3. Entropy and error locality. (a) Incorrect solutions exhibit higher entropy than correct ones. (b) The entropy distribution is heavily skewed toward zero; most tokens have (near-)zero entropy. (c) Neighborhoods around the first harmful token show higher mean entropy than overall entropy distribution, indicating that errors often arise from locally uncertain regions.

3.3. RL-based Routing with Latency-aware Reward

Beyond entropy-guided stitching, we propose **R-Stitch⁺**, an RL extension of R-Stitch. At each decoding step, when the token entropy exceeds the threshold τ , the hidden state of the current model is fed into a lightweight router, which decides whether to continue with the SLM or switch to the LLM. Low-entropy tokens are always delegated to the SLM.

Reward design. The reward is decomposed into an accuracy term and an efficiency term:

$$R = r_{\text{acc}} + r_{\text{eff}}. \quad (3)$$

The accuracy reward r_{acc} reflects whether the final prediction is correct, while the efficiency reward r_{eff} penalizes computational cost. Unlike prior RL approaches for chain-of-thought reasoning that approximate efficiency by the number of generated tokens (Aggarwal & Welleck, 2025), such a proxy is unsuitable here: (i) we involve both a small and a large model, whose per-token costs differ significantly; and (ii) our framework allows partial-prefill operations, whose cost depends jointly on the KV cache size and the length of the newly prefilling span. Ideally, the most faithful measure of efficiency is the actual trajectory latency, so we define

$$r_{\text{eff}} = -\lambda \cdot r_{\text{acc}} \cdot \widehat{L}, \quad (4)$$

where \widehat{L} denotes trajectory latency and λ is a trade-off coefficient. Latency is penalized only when the output is correct, ensuring that the router does not pursue speed at the expense of accuracy.

Latency estimator. However, directly measuring wall-clock latency during RL rollouts is impractical: trajectories are executed in batches and per-trajectory profiling would incur prohibitive overhead. To address this, we first sample a set of prefilling and decoding operations for each model (SLM and LLM) under different input lengths and KV cache size, and fit their latency profiles via linear regression. Let N_{inf} denote

the number of tokens processed at the current step and N_{kv} the size of the KV cache before this step. The dominant cost arises from attention, which scales as $\mathcal{O}(N_{\text{inf}} \cdot N_{\text{kv}} + N_{\text{inf}}^2)$, plus linear terms in N_{inf} . Accordingly, we model the latency for a prefill operation as

$$T_{\text{prefill}}(N_{\text{inf}}, N_{\text{kv}}) = a \cdot N_{\text{inf}} \cdot N_{\text{kv}} + b \cdot N_{\text{inf}}^2 + c \cdot N_{\text{inf}} + d, \quad (5)$$

where coefficients (a, b, c, d) are fitted via linear regression on profiling data. A decoding step corresponds to $N_{\text{inf}} = 1$, yielding

$$T_{\text{decode}}(N_{\text{kv}}) = c \cdot N_{\text{kv}} + d. \quad (6)$$

The trajectory-level latency \widehat{L} is then obtained by summing the step-wise estimates.

DAPO optimization. We train the router with the DAPO optimizer (Yu et al., 2025). For each prompt (q, a) , we sample a group of G routed trajectories $\{o_i\}_{i=1}^G \sim \pi_{\theta_{\text{old}}}(\cdot | q)$ and compute a scalar reward R_i for each trajectory. Let $o_{i,t}$ be the t -th action in o_i . We define the importance ratio and the group-normalized advantage as

$$r_{i,t}(\theta) = \frac{\pi_{\theta}(o_{i,t} | q, o_{i,<t})}{\pi_{\theta_{\text{old}}}(o_{i,t} | q, o_{i,<t})}, \quad (7)$$

$$\widehat{A}_{i,t} = \frac{R_i - \text{mean}(\{R_j\}_{j=1}^G)}{\text{std}(\{R_j\}_{j=1}^G)}.$$

Here, $\pi_{\theta}(\cdot)$ represents the current router policy, while $\pi_{\theta_{\text{old}}}(\cdot)$ denotes the policy used to sample trajectories in the previous iteration. Let $\text{clip}_{\varepsilon}(x) = \min(\max(x, 1 - \varepsilon), 1 + \varepsilon)$ denote the clipping operator. The DAPO objective is

$$\mathcal{J}_{\text{DAPO}}(\theta) = \mathbb{E}_{(q,a), \{o_i\} \sim \pi_{\theta_{\text{old}}}} \left[\frac{1}{\sum_{i=1}^G |o_i|} \sum_{i=1}^G \sum_{t=1}^{|o_i|} \min \left(r_{i,t}(\theta) \widehat{A}_{i,t}, \text{clip}_{\varepsilon}(r_{i,t}(\theta)) \widehat{A}_{i,t} \right) \right] \quad (8)$$

Table 1. Comparison of decoding strategies on five mathematical reasoning datasets. We report accuracy, latency (s/sample), and relative speedup (computed against the corresponding full LLM decoding) under decoding budgets of 8k and 16k tokens. **LLM-7B**, **LLM-14B**, and **LLM-32B** denote DeepSeek-R1-Distill-Qwen-7B, DeepSeek-R1-Distill-Qwen-14B, and QWQ-32B, respectively. **SLM** refers to L1-1.5B-Short (Liu et al., 2025), and **SpecDec** denotes speculative decoding using the corresponding models. Speedup is defined per LLM, per budget, per dataset as $\text{Lat}(\text{LLM})/\text{Lat}(\text{Method})$.

Method	τ	AIME			AMC			Minerva			MATH			OlympiadBench		
		Acc \uparrow	Lat. \downarrow	Spd. \uparrow	Acc \uparrow	Lat. \downarrow	Spd. \uparrow	Acc \uparrow	Lat. \downarrow	Spd. \uparrow	Acc \uparrow	Lat. \downarrow	Spd. \uparrow	Acc \uparrow	Lat. \downarrow	Spd. \uparrow
Decoding budget = 8k tokens																
SLM	–	10.00	5.91	–	50.60	5.37	–	25.37	5.03	–	73.60	4.56	–	36.89	5.42	–
LLM-7B	–	33.33	86.63	1.00 \times	66.27	63.15	1.00 \times	31.62	41.79	1.00 \times	86.00	38.34	1.00 \times	51.85	117.31	1.00 \times
SpecDec	–	36.67	201.23	0.43 \times	69.88	95.42	0.66 \times	34.19	56.59	0.74 \times	87.00	48.71	0.79 \times	51.85	134.23	0.87 \times
R-Stitch	0.001	36.67	89.86	0.96 \times	77.11	58.72	1.08 \times	34.19	38.73	1.08 \times	89.40	32.94	1.16 \times	55.26	105.29	1.11 \times
R-Stitch	0.02	40.00	62.03	1.40 \times	69.88	34.89	1.81 \times	33.09	18.98	2.20 \times	87.00	16.61	2.31 \times	51.85	70.43	1.67 \times
R-Stitch	0.03	30.00	42.06	1.84 \times	69.88	24.55	2.57 \times	33.09	15.07	2.77 \times	85.60	15.15	2.53 \times	48.59	51.43	2.28 \times
R-Stitch ⁺	–	40.00	37.19	2.33 \times	68.67	21.08	3.00 \times	35.29	15.33	2.73 \times	86.60	15.68	2.45 \times	52.00	45.02	2.34 \times
LLM-14B	–	43.33	153.20	1.00 \times	68.67	101.76	1.00 \times	35.29	48.02	1.00 \times	86.00	41.66	1.00 \times	54.07	190.89	1.00 \times
SpecDec	–	50.00	139.10	1.10 \times	68.67	95.59	1.06 \times	34.93	53.02	0.91 \times	82.80	45.88	0.91 \times	54.22	180.03	1.06 \times
R-Stitch	0.001	50.00	129.88	1.18 \times	69.88	79.54	1.28 \times	35.66	40.54	1.18 \times	89.00	37.03	1.13 \times	54.22	165.07	1.16 \times
R-Stitch	0.02	43.33	87.61	1.75 \times	69.88	41.82	2.43 \times	35.66	22.16	2.17 \times	85.20	20.53	2.05 \times	52.44	96.09	1.99 \times
R-Stitch	0.03	43.33	61.59	2.49 \times	68.67	26.43	3.85 \times	34.93	17.59	2.73 \times	83.40	14.77	2.82 \times	48.44	52.36	3.65 \times
R-Stitch ⁺	–	50.00	107.19	1.43 \times	73.49	49.91	2.04 \times	35.66	26.66	1.80 \times	88.20	29.08	1.43 \times	56.30	108.67	1.76 \times
LLM-32B	–	43.33	354.85	1.00 \times	60.24	292.78	1.00 \times	41.18	231.10	1.00 \times	87.53	178.38	1.00 \times	50.67	379.52	1.00 \times
SpecDec	–	40.00	270.25	1.31 \times	59.04	209.72	1.40 \times	41.91	182.28	1.27 \times	88.60	136.73	1.30 \times	50.04	351.27	1.08 \times
R-Stitch	0.001	50.00	261.86	1.40 \times	68.75	209.88	1.39 \times	42.65	141.24	1.64 \times	91.20	95.49	1.87 \times	50.67	341.67	1.11 \times
R-Stitch	0.02	50.00	184.97	1.92 \times	68.67	118.26	2.48 \times	36.76	59.58	3.87 \times	89.80	43.49	4.10 \times	53.78	226.71	1.67 \times
R-Stitch	0.03	40.00	178.19	1.99 \times	69.88	86.88	3.37 \times	34.56	43.41	5.32 \times	87.00	32.21	5.54 \times	52.15	157.47	2.41 \times
Decoding budget = 16k tokens																
SLM	–	10.00	5.91	–	50.60	5.37	–	25.37	5.03	–	73.60	4.56	–	36.89	5.42	–
LLM-7B	–	40.00	195.77	1.00 \times	71.08	116.41	1.00 \times	34.93	54.43	1.00 \times	90.80	50.07	1.00 \times	58.67	208.77	1.00 \times
SpecDec	–	50.00	258.54	0.76 \times	80.72	132.45	0.88 \times	35.66	115.76	0.47 \times	91.20	44.47	1.13 \times	60.15	267.03	0.78 \times
R-Stitch	0.001	46.67	192.22	1.03 \times	80.72	97.26	1.20 \times	35.66	45.53	1.20 \times	91.00	38.34	1.31 \times	60.15	201.13	1.04 \times
R-Stitch	0.02	50.00	110.16	1.78 \times	67.47	54.17	2.15 \times	33.09	18.79	2.90 \times	88.60	22.56	2.22 \times	58.67	109.98	1.90 \times
R-Stitch	0.03	36.67	41.51	4.72 \times	66.27	38.07	3.06 \times	35.29	13.50	4.03 \times	83.20	15.62	3.21 \times	54.22	65.65	3.18 \times
R-Stitch ⁺	–	50.00	86.03	2.28 \times	77.11	56.03	2.08 \times	35.29	13.68	3.98 \times	88.60	16.02	3.13 \times	59.11	95.31	2.19 \times
LLM-14B	–	50.00	246.95	1.00 \times	86.75	146.51	1.00 \times	39.34	68.99	1.00 \times	88.60	66.54	1.00 \times	60.00	316.06	1.00 \times
SpecDec	–	50.00	275.64	0.90 \times	83.13	138.53	1.06 \times	39.34	55.40	1.25 \times	87.40	67.18	0.99 \times	60.00	360.14	1.05 \times
R-Stitch	0.001	56.67	217.06	1.14 \times	79.52	90.72	1.61 \times	37.87	40.46	1.70 \times	89.40	39.82	1.67 \times	61.06	290.20	1.09 \times
R-Stitch	0.02	43.33	99.12	2.49 \times	66.27	51.29	2.86 \times	31.99	22.74	3.04 \times	87.80	22.62	2.94 \times	54.22	108.61	2.91 \times
R-Stitch	0.03	40.00	54.89	4.50 \times	63.86	28.38	5.16 \times	33.82	16.14	4.27 \times	84.80	17.37	3.83 \times	48.59	68.63	4.61 \times
R-Stitch ⁺	–	53.33	132.98	1.86 \times	79.52	68.50	2.14 \times	37.13	35.11	1.96 \times	89.60	33.70	1.97 \times	59.11	121.39	2.60 \times
LLM-32B	–	56.67	591.67	1.00 \times	87.95	419.94	1.00 \times	46.69	348.48	1.00 \times	94.00	249.92	1.00 \times	67.70	722.77	1.00 \times
SpecDec	–	70.00	526.03	1.12 \times	87.95	326.73	1.29 \times	44.23	273.07	1.28 \times	93.20	187.79	1.33 \times	67.70	798.23	0.90 \times
R-Stitch	0.001	70.00	488.87	1.21 \times	90.36	288.92	1.45 \times	41.18	126.62	2.75 \times	94.00	172.08	1.45 \times	66.07	654.24	1.10 \times
R-Stitch	0.02	50.00	333.17	1.78 \times	81.93	168.19	2.50 \times	40.07	73.32	4.75 \times	90.60	80.21	3.12 \times	61.19	358.87	2.01 \times
R-Stitch	0.03	53.33	276.03	2.14 \times	73.49	143.53	2.93 \times	36.40	43.58	8.00 \times	87.80	38.32	6.52 \times	55.70	209.96	3.44 \times

where ε is the clipping threshold.

4. Experiments

Implementation details. We evaluate our proposed method on five mathematical reasoning benchmarks: Olympiad-Bench (He et al., 2024a), AIME (Li et al., 2024a), Minerva (Lewkowycz et al., 2022), AMC (Li et al., 2024a), and MATH (Hendrycks et al., 2021). We adopt DeepSeek-Math-R1-Distill-Qwen models at 7B and 14B scales, and QwQ-32B as the 32B-scale LLM, with L1-Short serving as the SLM. Our method is implemented within the vLLM (Kwon et al., 2023) inference framework, where the LLM and SLM are instantiated as separate engines, each maintaining its own key-value cache to enable independent decoding and efficient model switching. Speculative decoding baselines

are evaluated using the official vLLM speculative decoding code. For R-Stitch⁺, we train the router using DAPO (Yu et al., 2025)’s publicly released RL training dataset, with $\lambda = 5 \times 10^{-6}$, $\tau = 0.001$, batch size 32, and rollout group size 8. The latency estimator is calibrated in milliseconds. Due to GPU memory constraints, RL experiments are conducted only on the 7B and 14B models. All latency numbers reported in the results correspond to the average wall-clock inference time per sample on a single NVIDIA A100 GPU with batch size 1.

Main results on math reasoning benchmarks. We evaluate R-Stitch under entropy thresholds $\tau \in \{0.001, 0.02, 0.03\}$, comparing against SLM-only decoding, full LLM decoding, and speculative decoding (SpecDec). Table 1 reports accuracy, latency, and rela-

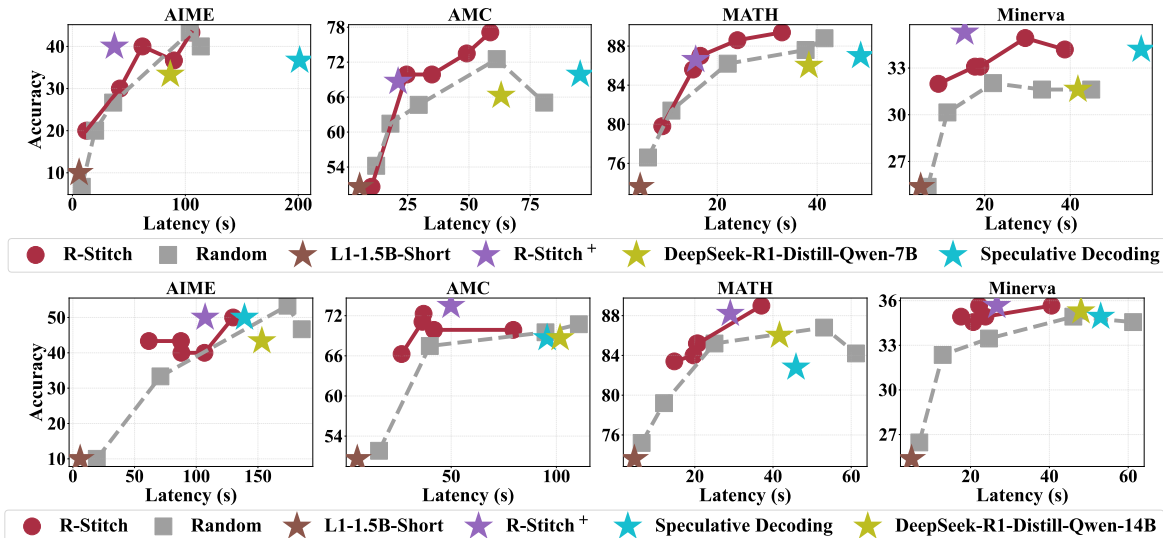


Figure 4. Accuracy–latency trade-off curves on mathematical reasoning datasets. The first row uses the 7B LLM, and the second row uses the 14B LLM. The red lines correspond to our method (R-Stitch) under varying entropy thresholds τ and a random routing baseline.

tive speedup across five mathematical reasoning benchmarks under decoding budgets of 8k and 16k tokens. Overall, R-Stitch consistently reduces latency with minimal accuracy degradation relative to full LLM decoding. At $\tau = 0.02$, LLM-7B achieves $1.4\times\text{--}2.3\times$ speedups at 8k and $1.7\times\text{--}2.9\times$ at 16k, while maintaining accuracy close to the LLM baseline. For larger models, efficiency gains become more pronounced: LLM-14B reaches $1.7\times\text{--}2.4\times$ at 8k and up to $3.0\times$ at 16k, while LLM-32B attains speedups of $1.9\times\text{--}4.1\times$ at 8k and $1.8\times\text{--}4.8\times$ at 16k. In particular, the observed accuracy gains arise because R-Stitch shortens overly verbose LLM reasoning traces, preventing truncation under strict length budgets and thereby avoiding accuracy degradation. SpecDec shows mixed performance: while occasionally competitive, it often runs slower than standard LLM decoding (e.g., 7B at 8k) or sacrifices accuracy. This slowdown is largely due to frequent rejections under low model agreement, which cause the tokens of SLM to be discarded and re-decoded by the LLM, resulting in more total decoding steps than even vanilla LLM decoding. SLM-only decoding remains fastest but yields substantially lower accuracy, highlighting the necessity of hybrid approaches. These results demonstrate that entropy-based routing provides a robust trade-off between efficiency and accuracy across different model scales and token budgets, with larger models benefiting the most in relative speedups.

Latency–accuracy trade-off. We further assess entropy-guided routing by varying the threshold $\tau \in \{0.001, 0.005, 0.02, 0.03, 0.05\}$ and reporting the resulting accuracy–latency trade-off. As baselines, we consider random routing, where tokens are assigned to the SLM with fixed probabilities $p \in \{0.1, 0.3, 0.5, 0.7, 0.9\}$, along with fixed decoding strategies including SLM-only, LLM-only,

and speculative decoding. Figure 4 presents results on four mathematical reasoning benchmarks with both 7B and 14B LLMs. Across all settings, R-Stitch consistently outperforms random routing, confirming entropy as a reliable confidence signal. On relatively simple tasks such as AMC, it achieves accuracy comparable to full LLM decoding while operating at substantially lower latency. Overall, entropy-based routing offers a simple, training-free mechanism that effectively balances efficiency and accuracy across diverse datasets and model scales. In addition, by tuning the entropy threshold, R-Stitch naturally adapts to different computational budgets without retraining, enabling practitioners to approach optimal accuracy under varying latency constraints.

Per-sample comparison with Speculative Decoding. Figure 5 provides per-sample visualizations of latency speedup and token reduction when applying R-Stitch⁺ and Speculative Decoding on the LLM-7B in AMC. We observe that R-Stitch⁺ consistently accelerates the majority of samples, while Speculative Decoding only yields speedup on a small portion of samples and causes slowdowns on most due to consistency issues. Notably, the theoretical upper bound of speculative decoding’s speedup under high consistency is the latency ratio between the LLM and SLM. In the visualization, the fastest sample achieves just above a $2\times$ speedup, which matches the decoding latency gap between the 7B and 1.5B models. *In contrast, our method additionally leverages the concise expressiveness of the SLM while preserving accuracy, thereby achieving substantially higher acceleration of up to $14\times$.*

Memory Overhead of Dual KV Caches. R-Stitch, like all speculative-decoding–style approaches, maintains separate KV caches for the SLM and LLM. To quantify the actual

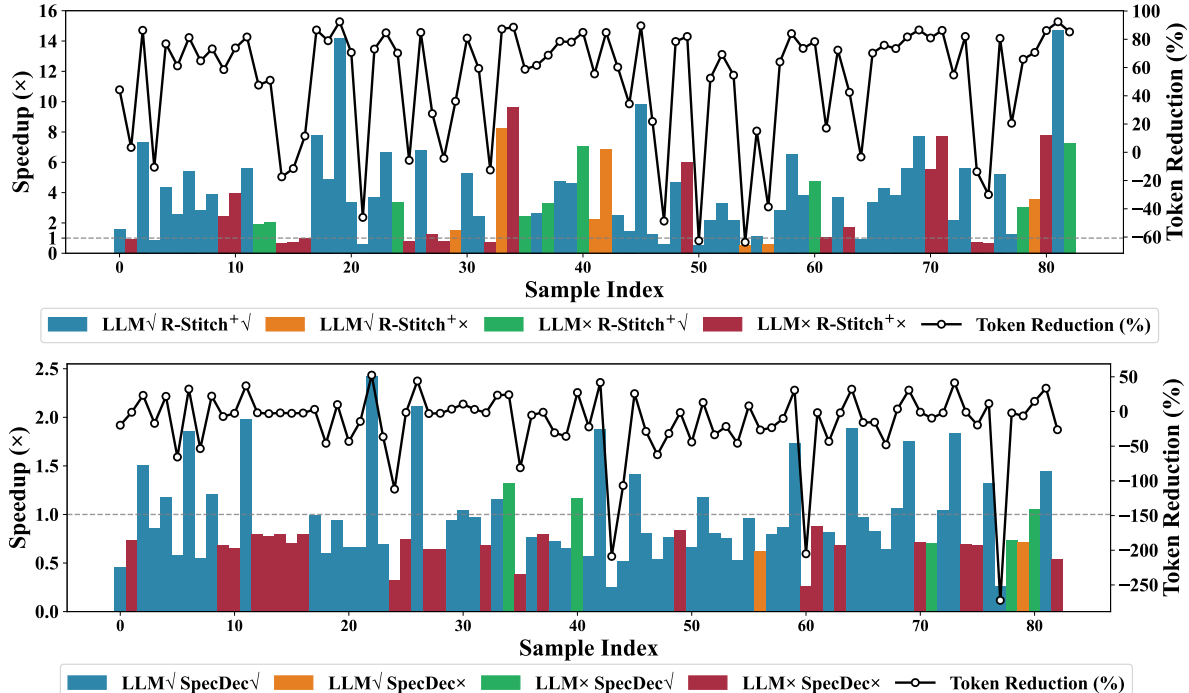


Figure 5. Per-sample visualization of R-Stitch⁺ and Speculative Decoding (LLM-7B). Each bar shows the latency speedup of one sample relative to the baseline LLM. Bar colors encode correctness outcomes of the baseline and R-Stitch⁺. The dashed horizontal line at 1 indicates no speedup. The black solid curve with hollow-circle markers represents token reduction percentages per sample.

Table 2. Memory usage of SLM/LLM models and their KV caches under BF16. **KV/tok** denotes per-token KV cache size in MB, **Wts** denotes model weights in MB, and **Total@8k/Total@16k** report total memory usage at 8k/16k context lengths.

Model	KV/tok	Wts	Total@8k	Total@16k
1.5B	0.028	3036	3265	3494
7B	0.055	15640	16091	16542
14B	0.189	29275	30824	32374
32B	0.253	63890	65958	68026

overhead, we measure model weights and KV footprints in v_{LLM} under BF16 precision. Table 2 reports per-token KV size, model weights, and total memory usage at 8k and 16k context lengths. When paired with a 7B model under a 16k context, the 1.5B SLM introduces only a 17.44% memory increase, which further decreases to 9.74% for a 14B model and 4.89% for a 32B model. These results show that the additional memory required by R-Stitch remains modest relative to the LLM footprint, while enabling substantial end-to-end latency reductions.

5. Conclusion

This paper has introduced R-Stitch, a dynamic routing strategy for accelerating large language model inference by selectively delegating token-level computation to a SLM. Our method leverages an entropy-based switching mechanism

that routes easy tokens to the lightweight model while preserving overall output quality. This design enables a favorable trade-off between inference latency and accuracy without requiring additional retraining or architectural changes. Furthermore, we have extended this approach to R-Stitch⁺, which incorporates a reinforcement learning (RL)-based router trained with a latency-aware reward. By adaptively deciding when to switch between the SLM and the LLM, R-Stitch⁺ refines the efficiency-accuracy balance beyond fixed entropy thresholds, achieving stronger acceleration while maintaining high accuracy. Comprehensive experiments on multiple datasets have demonstrated that our framework achieves consistent improvements over static baselines and speculative decoding, offering a practical and efficient solution for real-world deployment of LLMs.

Limitations and future work. Our current implementation supports only batch size 1 due to dynamic token-level model switching, which restricts hardware utilization in practical deployment. Addressing this limitation may require designing new scheduling strategies or restructuring the routing mechanism to better accommodate batched inference. To further alleviate the KV cache and parameter burden from maintaining two models, we plan to adopt parameter-sharing strategies to enhance memory efficiency. These extensions could improve the robustness and scalability of dynamic model routing, and enable more fine-grained control over the latency-accuracy trade-off.

Impact Statement

This paper presents work aimed at advancing the field of machine learning by improving the efficiency of inference-time reasoning in large language models. The proposed method reduces computational cost and latency while maintaining accuracy, which may facilitate more efficient and accessible deployment of reasoning-capable models. The societal and ethical implications of this work are consistent with those commonly associated with improvements in machine learning efficiency, including potential benefits in sustainability and practical usability. The method operates purely at inference time and does not introduce new model capabilities, data sources, or application domains, and therefore does not raise new ethical concerns beyond those already well established for large language models. Overall, we do not identify any broader impacts that require specific discussion beyond these considerations.

References

- Aggarwal, P. and Welleck, S. L1: Controlling how long a reasoning model thinks with reinforcement learning. *arXiv preprint arXiv:2503.04697*, 2025.
- Ankner, Z., Parthasarathy, R., Nrusimha, A., Rinard, C., Ragan-Kelley, J., and Brandon, W. Hydra: Sequentially-dependent draft heads for medusa decoding. *arXiv preprint arXiv:2402.05109*, 2024.
- Austin, J., Odena, A., Nye, M., Bosma, M., Michalewski, H., Dohan, D., Jiang, E., Cai, C., Terry, M., Le, Q., et al. Program synthesis with large language models. *arXiv preprint arXiv:2108.07732*, 2021.
- Cai, T., Li, Y., Geng, Z., Peng, H., Lee, J. D., Chen, D., and Dao, T. Medusa: Simple llm inference acceleration framework with multiple decoding heads. In *ICML*, pp. 5209–5235, 2024.
- Chen, C., Borgeaud, S., Irving, G., Lespiau, J.-B., Sifre, L., and Jumper, J. Accelerating large language model decoding with speculative sampling. *arXiv preprint arXiv:2302.01318*, 2023.
- Chen, M., Tworek, J., Jun, H., Yuan, Q., Pinto, H. P. D. O., Kaplan, J., Edwards, H., Burda, Y., Joseph, N., Brockman, G., et al. Evaluating large language models trained on code. *arXiv preprint arXiv:2107.03374*, 2021.
- Cobbe, K., Kosaraju, V., Bavarian, M., Chen, M., Jun, H., Kaiser, L., Plappert, M., Tworek, J., Hilton, J., Nakano, R., et al. Training verifiers to solve math word problems. *arXiv preprint arXiv:2110.14168*, 2021.
- Fang, G., Ma, X., and Wang, X. Thinkless: Llm learns when to think. *arXiv preprint arXiv:2505.13379*, 2025.
- Fatemi, M., Rafiee, B., Tang, M., and Talamadupula, K. Concise reasoning via reinforcement learning. *arXiv preprint arXiv:2504.05185*, 2025.
- Gao, Y., Guo, S., Cao, S., Xia, Y., Wang, L., Ma, L., Sun, Y., Ye, T., Dong, L., So, H. K.-H., Hua, Y., Cao, T., Yang, F., and Yang, M. Seerattention-r: Sparse attention adaptation for long reasoning. *arXiv preprint arXiv:2506.08889*, 2025.
- Gema, A. P., Leang, J. O. J., Hong, G., Devoto, A., Mancino, A. C. M., Saxena, R., He, X., Zhao, Y., Du, X., Madani, M. R. G., et al. Are we done with mmlu? In *Proceedings of the 2025 Conference of the Nations of the Americas Chapter of the Association for Computational Linguistics: Human Language Technologies (Volume 1: Long Papers)*, pp. 5069–5096, 2025.
- Gu, A., Roziere, B., Leather, H. J., Solar-Lezama, A., Synnaeve, G., and Wang, S. Cruxeval: A benchmark for code reasoning, understanding and execution. In *ICML*.
- Guo, D., Yang, D., Zhang, H., Song, J., Zhang, R., Xu, R., Zhu, Q., Ma, S., Wang, P., Bi, X., et al. Deepseek-r1: Incentivizing reasoning capability in llms via reinforcement learning. *arXiv preprint arXiv:2501.12948*, 2025.
- He, C., Luo, R., Bai, Y., Hu, S., Thai, Z. L., Shen, J., Hu, J., Han, X., Huang, Y., Zhang, Y., et al. Olympiadbench: A challenging benchmark for promoting agi with olympiad-level bilingual multimodal scientific problems. *arXiv preprint arXiv:2402.14008*, 2024a.
- He, H., Pan, Z., Liu, J., Cai, J., and Zhuang, B. Efficient stitchable task adaptation. In *CVPR*, pp. 28555–28565, 2024b.
- Hendrycks, D., Burns, C., Kadavath, S., Arora, A., Basart, S., Tang, E., Song, D., and Steinhardt, J. Measuring mathematical problem solving with the math dataset. *arXiv preprint arXiv:2103.03874*, 2021.
- Hou, B., Zhang, Y., Ji, J., Liu, Y., Qian, K., Andreas, J., and Chang, S. Thinkprune: Pruning long chain-of-thought of llms via reinforcement learning. *arXiv preprint arXiv:2504.01296*, 2025.
- Hu, S., Li, J., Xie, X., Lu, Z., Toh, K.-C., and Zhou, P. Griffin: Effective token alignment for faster speculative decoding. *arXiv preprint arXiv:2502.11018*, 2025.
- Jain, N., Han, K., Gu, A., Li, W.-D., Yan, F., Zhang, T., Wang, S., Solar-Lezama, A., Sen, K., and Stoica, I. Livecodebench: Holistic and contamination free evaluation of large language models for code. In *ICLR*, 2025.
- Jiang, L., Wu, X., Huang, S., Dong, Q., Chi, Z., Dong, L., Zhang, X., Lv, T., Cui, L., and Wei, F. Think only

- when you need with large hybrid-reasoning models. *arXiv preprint arXiv:2505.14631*, 2025.
- Kojima, T., Gu, S. S., Reid, M., Matsuo, Y., and Iwasawa, Y. Large language models are zero-shot reasoners. *NeurIPS*, 35:22199–22213, 2022.
- Kwon, W., Li, Z., Zhuang, S., Sheng, Y., Zheng, L., Yu, C., Gonzalez, J., Zhang, H., and Stoica, I. vllm: Easy, fast, and cheap llm serving with pagedattention. <https://vllm.ai/> (accessed 9 August 2023), 2023.
- Lewkowycz, A., Andreassen, A., Dohan, D., Dyer, E., Michalewski, H., Ramasesh, V., Slone, A., Anil, C., Schlag, I., Gutman-Solo, T., et al. Solving quantitative reasoning problems with language models. *NeurIPS*, 35: 3843–3857, 2022.
- Li, D., Cao, S., Cao, C., Li, X., Tan, S., Keutzer, K., Xing, J., Gonzalez, J. E., and Stoica, I. S*: Test time scaling for code generation. *arXiv preprint arXiv:2502.14382*, 2025a.
- Li, J., Beeching, E., Tunstall, L., Lipkin, B., Soletskyi, R., Huang, S., Rasul, K., Yu, L., Jiang, A. Q., Shen, Z., et al. Numinamath: The largest public dataset in ai4maths with 860k pairs of competition math problems and solutions. *Hugging Face repository*, 13:9, 2024a.
- Li, Y., Wei, F., Zhang, C., and Zhang, H. Eagle: Speculative sampling requires rethinking feature uncertainty. In *ICML*, pp. 28935–28948, 2024b.
- Li, Y., Wei, F., Zhang, C., and Zhang, H. Eagle-2: Faster inference of language models with dynamic draft trees. In *EMNLP*, pp. 7421–7432, 2024c.
- Li, Y., Wei, F., Zhang, C., and Zhang, H. Eagle-3: Scaling up inference acceleration of large language models via training-time test. *arXiv preprint arXiv:2503.01840*, 2025b.
- Liao, B., Xu, Y., Dong, H., Li, J., Monz, C., Savarese, S., Sahoo, D., and Xiong, C. Reward-guided speculative decoding for efficient llm reasoning. In *Forty-second International Conference on Machine Learning*.
- Lin, B., Li, Z., Cheng, X., Niu, Y., Ye, Y., He, X., Yuan, S., Yu, W., Wang, S., Ge, Y., et al. Uniworld: High-resolution semantic encoders for unified visual understanding and generation. *arXiv preprint arXiv:2506.03147*, 2025.
- Lin, B. Y., Le Bras, R., Richardson, K., Sabharwal, A., Poovendran, R., Clark, P., and Choi, Y. ZebraLogic: On the scaling limits of llms for logical reasoning. In *ICML*.
- Liu, F., Tang, Y., Liu, Z., Ni, Y., Tang, D., Han, K., and Wang, Y. Kangaroo: Lossless self-speculative decoding for accelerating llms via double early exiting. *NeurIPS*, 37:11946–11965, 2024.
- Liu, H., Li, C., Wu, Q., and Lee, Y. J. Visual instruction tuning. *NeurIPS*, 36:34892–34916, 2023.
- Liu, Z., Chen, C., Li, W., Qi, P., Pang, T., Du, C., Lee, W. S., and Lin, M. Understanding r1-zero-like training: A critical perspective. *arXiv preprint arXiv:2503.20783*, 2025.
- Ma, W., He, J., Snell, C., Griggs, T., Min, S., and Zaharia, M. Reasoning models can be effective without thinking. *arXiv preprint arXiv:2504.09858*, 2025.
- Pan, X., Shukla, S. N., Singh, A., Zhao, Z., Mishra, S. K., Wang, J., Xu, Z., Chen, J., Li, K., Juefei-Xu, F., et al. Transfer between modalities with metaqueries. *arXiv preprint arXiv:2504.06256*, 2025a.
- Pan, Z., Cai, J., and Zhuang, B. Stitchable neural networks. In *CVPR*, pp. 16102–16112, 2023.
- Pan, Z., Liu, J., He, H., Cai, J., and Zhuang, B. Stitched vits are flexible vision backbones. In *ECCV*, pp. 258–274, 2024.
- Pan, Z., Zhuang, B., Huang, D.-A., Nie, W., Yu, Z., Xiao, C., Cai, J., and Anandkumar, A. T-stitch: Accelerating sampling in pre-trained diffusion models with trajectory stitching. In *ICLR*, 2025b.
- Rein, D., Hou, B. L., Stickland, A. C., Petty, J., Pang, R. Y., Dirani, J., Michael, J., and Bowman, S. R. Gpqa: A graduate-level google-proof q&a benchmark. In *COLM*, 2024.
- Sadhukhan, R., Chen, J., Chen, Z., Tiwari, V., Lai, R., Shi, J., Yen, I. E.-H., May, A., Chen, T., and Chen, B. Magicdec: Breaking the latency-throughput tradeoff for long context generation with speculative decoding. *arXiv preprint arXiv:2408.11049*, 2024.
- Tang, J., Zhao, Y., Zhu, K., Xiao, G., Kasikci, B., and Han, S. Quest: Query-aware sparsity for efficient long-context llm inference. *ICML*, 2024.
- Wei, J., Wang, X., Schuurmans, D., Bosma, M., Xia, F., Chi, E., Le, Q. V., Zhou, D., et al. Chain-of-thought prompting elicits reasoning in large language models. *NeurIPS*, 35: 24824–24837, 2022.
- Yang, A., Li, A., Yang, B., Zhang, B., Hui, B., Zheng, B., Yu, B., Gao, C., Huang, C., Lv, C., et al. Qwen3 technical report. *arXiv preprint arXiv:2505.09388*, 2025a.
- Yang, C., Si, Q., Duan, Y., Zhu, Z., Zhu, C., Li, Q., Lin, Z., Cao, L., and Wang, W. Dynamic early exit in reasoning models. *arXiv preprint arXiv:2504.15895*, 2025b.

- Yao, S., Yu, D., Zhao, J., Shafran, I., Griffiths, T., Cao, Y., and Narasimhan, K. Tree of thoughts: Deliberate problem solving with large language models. *NeurIPS*, 36:11809–11822, 2023.
- Yi, J., Wang, J., and Li, S. Shorterbetter: Guiding reasoning models to find optimal inference length for efficient reasoning. *arXiv preprint arXiv:2504.21370*, 2025.
- Yu, Q., Zhang, Z., Zhu, R., Yuan, Y., Zuo, X., Yue, Y., Dai, W., Fan, T., Liu, G., Liu, L., et al. Dapo: An open-source llm reinforcement learning system at scale. *arXiv preprint arXiv:2503.14476*, 2025.
- Zhang, J., Lin, N., Hou, L., Feng, L., and Li, J. Adaptthink: Reasoning models can learn when to think. *arXiv preprint arXiv:2505.13417*, 2025.
- Zhang, S., Chen, Z., Shen, Y., Ding, M., Tenenbaum, J. B., and Gan, C. Planning with large language models for code generation. In *ICLR*.
- Zhang, X., Du, C., Pang, T., Liu, Q., Gao, W., and Lin, M. Chain of preference optimization: Improving chain-of-thought reasoning in llms. *NeurIPS*, 37:333–356, 2024.
- Zhang, Z., Zhang, A., Li, M., and Smola, A. Automatic chain of thought prompting in large language models. In *ICLR*, 2023.
- Zheng, X., Lou, J., Cao, B., Wen, X., Ji, Y., Lin, H., Lu, Y., Han, X., Zhang, D., and Sun, L. Critic-cot: Boosting the reasoning abilities of large language model via chain-of-thoughts critic. *arXiv preprint arXiv:2408.16326*, 2024.

A. Appendix

A.1. Inference algorithm of the proposed method

Algorithm 1 Inference procedure of the proposed method

Require: Prompt x ; models SLM, LLM; threshold τ ; max length T_{\max}

- 1: Optional: router π_θ (R-Stitch⁺)
- 2: $KV^{\text{SLM}} \leftarrow \emptyset, KV^{\text{LLM}} \leftarrow \emptyset; L^{\text{SLM}} = L^{\text{LLM}} = 0 \triangleright KV^{\text{SLM}}, KV^{\text{LLM}}$: KV caches; $L^{\text{SLM}}, L^{\text{LLM}}$: KV cache sizes of SLM and LLM
- 3: $y \leftarrow [], \text{ACTIVE} \leftarrow \text{SLM} \triangleright y$: generated output; **ACTIVE**: current inference model
- 4: **for** $t = 1 \rightarrow T_{\max}$ **do**
- 5: **if** $L^{\text{ACTIVE}} < |x \oplus y|$ **then**
- 6: **Prefill:** run **ACTIVE** on $(x \oplus y)[L^{\text{ACTIVE}}:]$ to update cache and generate (\mathbf{p}_t, y_t) ; $L^{\text{ACTIVE}} \leftarrow |x \oplus y| + 1 \triangleright$ KV cache not up-to-date; \mathbf{p}_t : prob. distribution; y_t : generated token
- 7: **else**
- 8: **Decode:** run **ACTIVE** with cache to generate (\mathbf{p}_t, y_t) ; $L^{\text{ACTIVE}} \leftarrow L^{\text{ACTIVE}} + 1$
- 9: **end if**
- 10: Compute entropy \mathcal{H}_t from \mathbf{p}_t (Eq. 1) $\triangleright \mathcal{H}_t$: token entropy
- 11: **if** $\mathcal{H}_t > \tau$ **then**
- 12: **if** R-Stitch **then**
- 13: $\text{SWITCH} \leftarrow \text{True}$
- 14: **else if** R-Stitch⁺ **then**
- 15: $\text{SWITCH} \leftarrow (\arg \max_{a \in \{\text{SLM}, \text{LLM}\}} \pi_\theta(a | s_t) = \text{LLM}) \triangleright$ router decision (state s_t)
- 16: **end if**
- 17: **if** **ACTIVE** = SLM **and** **SWITCH** **then**
- 18: **Discard** y_t and rollback KV^{SLM} ; **ACTIVE** \leftarrow LLM; **continue** \triangleright switch SLM \rightarrow LLM, token not kept
- 19: **end if**
- 20: **else if** **ACTIVE** = LLM **then**
- 21: **ACTIVE** \leftarrow SLM \triangleright switch LLM \rightarrow SLM
- 22: **end if**
- 23: Append y_t to y ; update cache \triangleright append only if token not discarded
- 24: **if** $y_t = [\text{EOS}]$ **then**
- 25: **break**
- 26: **end if**
- 27: **end for**
- 28: **return** y

A.2. Latency Regression Results

Building on the latency estimator introduced in Eq. 5 and Eq. 6, we report the fitted coefficients (a, b, c, d) obtained from profiling three representative models: SLM-1.5B, LLM-7B, and LLM-14B. Recall that N_{inf} denotes the number of tokens processed at the current step and N_{kv} the size of the KV cache before this step. Latency is modeled as

$$T(N_{\text{inf}}, N_{\text{kv}}) = a \cdot N_{\text{inf}} \cdot N_{\text{kv}} + b \cdot N_{\text{inf}}^2 + c \cdot N_{\text{inf}} + d.$$

The fitted functions are as follows (latency T in milliseconds):

- SLM-1.5B:

$$T(N_{\text{inf}}, N_{\text{kv}}) = 0.000021 \cdot (N_{\text{inf}} \cdot N_{\text{kv}}) + 0.000231 \cdot N_{\text{inf}}^2 - 0.121046 \cdot N_{\text{inf}} + 27.090929$$

- LLM-7B:

$$T(N_{\text{inf}}, N_{\text{kv}}) = 0.000027 \cdot (N_{\text{inf}} \cdot N_{\text{kv}}) + 0.000031 \cdot N_{\text{inf}}^2 - 0.045256 \cdot N_{\text{inf}} + 27.040801$$

- LLM-14B:

$$T(N_{\text{inf}}, N_{\text{kv}}) = 0.000045 \cdot (N_{\text{inf}} \cdot N_{\text{kv}}) + 0.000123 \cdot N_{\text{inf}}^2 - 0.082998 \cdot N_{\text{inf}} + 45.118931$$

These regression results provide practical estimators for per-step latency under varying input lengths and KV cache sizes, enabling efficient evaluation without costly profiling.

A.3. Related work of optimizing Speculative decoding

Recent approaches to speculative decoding acceleration can be understood as attempts to train auxiliary mechanisms that increase the consistency between the draft model and the target model. This line of research is exemplified by the EAGLE family and Griffin, while Hydra represents a lighter-weight but still consistency-oriented variant, and CITER departs somewhat from this trend but nevertheless introduces additional training cost. We briefly review these methods below.

EAGLE. The EAGLE series (Li et al., 2024b;c; 2025b) develops progressively more sophisticated training strategies for draft models. The original EAGLE (Li et al., 2024b) proposed to autoregressively predict the top-layer hidden features of the target model, rather than tokens directly, thereby anchoring the draft model’s outputs more closely to the target distribution. This was combined with a tree-based drafting mechanism and corresponding tree attention to improve parallelism. EAGLE-2 (Li et al., 2024c) extended this by introducing a dynamic draft tree that adapts its expansion based on the draft model’s confidence, reducing wasted computation on unlikely branches. Finally, EAGLE-3 (Li et al., 2025b) removed the restriction of feature-level prediction and returned to token-level generation, but enhanced it with multi-level feature fusion and a novel training-time test technique, which simulates self-feedback during training. These changes allow EAGLE-3 to scale better with more training data and to reach higher acceptance rates, but all variants require substantial supervised training of the draft model.

Griffin. Griffin (Hu et al., 2025) addresses the bottleneck of speculative decoding by improving the quality of the small draft model rather than modifying the large model or the verification process. It introduces guidance distillation to better align the draft model’s predictive distribution with that of the target model, and augments the architecture with lightweight enhancements that increase expressiveness without incurring significant cost. As a result, Griffin achieves substantially higher acceptance rates than naive draft models, thereby unlocking more consistent acceleration for speculative decoding.

Hydra. Hydra (Ankner et al., 2024) departs from training a separate small model and instead equips the large model with a set of Hydra heads, lightweight proposal modules attached to intermediate hidden states. Unlike the earlier Medusa framework (Cai et al., 2024), where draft heads were independent and predicted tokens in parallel, Hydra enforces sequential dependency across heads: each head conditions on the tokens predicted by previous heads. This design increases the internal consistency of the drafted sequence, leading to higher acceptance rates without the need for an external small model. Hydra thus offers a lighter-weight solution, but it still shares the central assumption that greater draft–target consistency is the key to efficiency.

Distinctive perspective of our method. In contrast to all these approaches, our work takes a fundamentally different perspective. We do not attempt to make the small and large models more consistent, nor do we introduce training overhead for rewriting. Instead, we explicitly exploit the insight that the small model is *simpler and naturally inconsistent* with the large model. Rather than mitigating this inconsistency, we turn it into an advantage, showing that it can be directly leveraged to improve speculative decoding efficiency. Training-free R-Stitch requires *no additional training* and no auxiliary modules, yet achieves significant acceleration. This reveals a new perspective: sometimes inconsistency between models is not a limitation to be avoided, but a property that can be actively harnessed for efficiency gains.

A.4. Comparison with State-of-the-Art Speculative Decoding

Table 3 compares our method with Eagle-3, the state-of-the-art speculative decoding approach reported in the official vLLM repository, on Qwen3-8B and Qwen3-14B across four mathematical reasoning benchmarks under both 8k and 16k decoding budgets. Both Eagle-3 and R-Stitch exploit the advantage that small models decode tokens faster than the LLM, thereby reducing per-token complexity. However, R-Stitch additionally leverages the conciseness of SLM outputs: by selectively retaining short, low-entropy continuations from the SLM, it reduces the overall output length, yielding substantially higher end-to-end acceleration. Notably, Eagle-3 employs a heavily trained draft model much smaller than our 1.5B SLM, making its per-token decoding inherently faster. Despite this disadvantage, R-Stitch achieves consistently larger speedups across all benchmarks and budgets, highlighting the benefit of flexible entropy-guided collaboration over purely consistency-driven speculative decoding.

A.5. Combining with Early Exit Strategies

We further examine whether R-Stitch can complement training-free early-exit methods to improve decoding efficiency. Specifically, we combine R-Stitch with DEER (Yang et al., 2025b), which halts generation once the model’s confidence surpasses a predefined threshold. As shown in Table 4, evaluated on MATH (Hendrycks et al., 2021), AIME (Li et al., 2024a),

Table 3. Performance comparison with the state-of-the-art speculative decoding baseline (Eagle-3, the fastest method reported in the official vLLM repository) on Qwen3-8/14B (Yang et al., 2025a) across four mathematical reasoning benchmarks. We report accuracy (Acc), latency (s/sample), average output length (Tok.), and relative speedup (Spd.), under both 8k-token and 16k-token decoding budgets.

Method	τ	AIME				AMC				Minerva				MATH			
		Acc \uparrow	Lat. \downarrow	Tok. \downarrow	Spd. \uparrow	Acc \uparrow	Lat. \downarrow	Tok. \downarrow	Spd. \uparrow	Acc \uparrow	Lat. \downarrow	Tok. \downarrow	Spd. \uparrow	Acc \uparrow	Lat. \downarrow	Tok. \downarrow	Spd. \uparrow
Decoding budget = 8k tokens																	
Qwen3-8B	–	30.00	97.50	7589.33	1.00 \times	59.04	81.68	6384.39	1.00 \times	34.93	68.49	5367.97	1.00 \times	84.00	56.02	4423.09	1.00 \times
Eagle-3	–	36.67	64.87	7740.33	1.50 \times	59.04	52.35	6575.19	1.56 \times	36.03	42.30	5380.57	1.62 \times	86.00	33.87	4437.59	1.65 \times
R-Stitch	0.001	50.00	64.89	6978.97	1.50 \times	71.08	44.72	4942.05	1.83 \times	42.65	35.68	3913.13	1.92 \times	89.60	24.77	2845.66	2.26 \times
R-Stitch	0.01	56.67	48.30	5527.50	2.02 \times	62.65	27.53	3316.34	2.97 \times	38.97	27.53	2030.41	2.49 \times	87.00	12.52	1614.31	4.47 \times
R-Stitch	0.02	26.67	39.35	4701.90	2.48 \times	66.27	19.27	2453.30	2.97 \times	34.56	10.86	1416.57	6.31 \times	83.60	9.27	1260.76	6.04 \times
Qwen3-14B	–	40.00	158.80	7549.47	1.00 \times	62.65	126.86	6055.57	1.00 \times	41.54	100.52	4808.01	1.00 \times	89.00	82.93	3980.87	1.00 \times
Eagle-3	–	43.33	110.48	7700.53	1.44 \times	60.24	83.70	6125.43	1.52 \times	39.71	67.10	4891.85	1.50 \times	88.20	53.89	4056.89	1.54 \times
R-Stitch	0.001	46.67	94.97	7043.47	1.67 \times	67.47	63.13	4802.56	2.01 \times	45.59	46.30	3545.74	2.17 \times	90.00	32.62	2688.23	2.54 \times
R-Stitch	0.01	43.33	75.51	6213.47	2.10 \times	65.06	35.75	3213.11	3.55 \times	40.44	20.53	1815.11	4.90 \times	88.00	16.24	1569.15	5.11 \times
R-Stitch	0.02	33.33	55.20	4836.30	2.88 \times	61.45	23.99	2330.29	5.29 \times	37.13	13.01	1266.13	7.73 \times	84.60	11.64	1223.35	7.12 \times
Decoding budget = 16k tokens																	
Qwen3-8B	–	63.33	156.21	11899.80	1.00 \times	81.93	115.33	9022.71	1.00 \times	47.43	90.28	6822.03	1.00 \times	94.40	65.05	5067.67	1.00 \times
Eagle-3	–	66.67	110.23	12080.73	1.42 \times	81.93	76.55	9008.47	1.51 \times	47.06	58.49	6981.51	1.54 \times	95.60	40.60	5150.57	1.60 \times
R-Stitch	0.0005	70.00	109.82	10942.50	1.42 \times	81.93	70.46	7107.68	1.64 \times	46.32	48.65	3640.69	1.86 \times	94.60	33.64	3640.69	1.93 \times
R-Stitch	0.001	60.00	102.83	10135.03	1.52 \times	74.70	65.14	6606.36	1.77 \times	41.54	44.73	4510.72	2.02 \times	94.80	29.20	3238.44	2.23 \times
R-Stitch	0.01	53.33	69.63	7506.93	2.24 \times	73.49	38.13	4319.67	3.02 \times	37.50	18.04	2142.44	5.00 \times	89.60	14.97	1839.84	4.35 \times
Qwen3-14B	–	70.00	248.17	11237.64	1.00 \times	81.93	167.32	7896.86	1.00 \times	46.69	125.74	5959.92	1.00 \times	95.60	94.76	4528.12	1.00 \times
Eagle-3	–	63.33	189.59	11203.67	1.31 \times	85.54	121.30	8292.41	1.38 \times	47.06	84.50	5930.95	1.49 \times	95.40	63.31	4616.20	1.50 \times
R-Stitch	0.0005	70.00	139.11	9637.84	1.78 \times	85.54	89.25	6346.75	1.87 \times	45.96	59.48	4373.63	2.11 \times	94.60	45.60	3427.84	2.08 \times
R-Stitch	0.001	70.00	136.51	9556.70	1.82 \times	83.13	91.11	6713.41	1.84 \times	44.85	53.10	3985.24	2.37 \times	94.20	37.34	3003.98	2.54 \times
R-Stitch	0.01	56.67	113.50	8668.10	2.19 \times	71.08	40.84	3512.52	4.10 \times	38.24	24.58	2116.48	5.12 \times	88.60	20.65	1868.24	4.59 \times

Table 4. Effect of applying R-Stitch ($\tau = 0.01$) on top of DEER with the LLM-7B under a 16k-token decoding budget. Accuracy (%), average token count, and inference latency (s) are reported. Results of the vanilla LLM-7B are also included for reference.

Dataset	LLM-7B			+ DEER			+ DEER + R-Stitch		
	Acc. (%)	Token	Lat. (s)	Acc. (%)	Token	Lat. (s)	Acc. (%)	Token	Lat. (s)
MATH	90.80	3381.51	50.07	89.20	2284.52	35.47	88.40	1564.90	20.59
AIME	40.00	11739.10	195.77	36.67	9229.03	210.37	36.67	4425.20	92.52
GSM8K	88.93	1398.54	20.91	90.07	698.47	9.69	90.07	462.41	6.76
GPQA-D	23.74	10134.81	171.76	27.78	7084.15	117.50	30.81	1047.85	18.15

GSM8K (Cobbe et al., 2021), and GPQA-D (Rein et al., 2024) under a 16k-token budget, the hybrid system substantially reduces both token count and end-to-end latency compared to DEER alone, while maintaining comparable accuracy. On AIME, token usage is reduced by more than 50% and latency drops from 210.37s to 92.52s, without affecting accuracy. On GPQA-D, the benefits are even more pronounced: latency decreases from 117.50s to 18.15s, while accuracy improves from 27.78% to 30.81%. Compared to vanilla LLM-7B decoding (171.76s), this corresponds to a 9.5 \times acceleration. These results confirm that early exiting and entropy-guided routing are complementary: DEER shortens the reasoning trajectory, whereas R-Stitch lowers per-token cost by selectively invoking the LLM only when needed. Together, they provide strictly greater efficiency by simultaneously addressing sequence length and per-step computation. For fairness, both +DEER and +DEER+R-Stitch results are reproduced using the official vLLM-based implementation of DEER, where the full context is re-filled after each early-exit decision. This design substantially underestimates the achievable efficiency gains, limiting the apparent acceleration of both DEER alone and our combined method. Our integration retains DEER’s stopping criterion but substitutes its single-model decoding with R-Stitch, ensuring that the reported improvements are attributable to our method.

A.6. Performance on code generation benchmarks.

Table 5 reports accuracy, latency, and relative speedup on programming benchmarks including LiveCodeBench (Jain et al., 2025), MBPP (Austin et al., 2021), and HumanEval (Chen et al., 2021). Compared to math reasoning, acceleration on code generation is more modest: when targeting accuracy comparable to the full LLM, the achievable latency reduction is limited. We attribute this to the characteristics of the specific SLM used in our study, which, while effective on math reasoning tasks, produces less concise and less reliable traces for code. This constrains the gains realizable from hybrid decoding on code

Table 5. Comparison of decoding strategies on three code generation benchmarks. We report accuracy, latency (s/sample), and relative speedup (computed against the corresponding full LLM decoding). LLM-7B and LLM-14B denote DeepSeek-R1-Distill-Qwen-7B and DeepSeek-R1-Distill-Qwen-14B, respectively. SLM refers to L1-1.5B-Short (Liu et al., 2025), and SpecDec denotes speculative decoding using the corresponding LLM.

Method	τ	LiveCodeBench			MBPP			HumanEval			Average		
		Acc \uparrow	Lat. \downarrow	Spd. \uparrow	Acc \uparrow	Lat. \downarrow	Spd. \uparrow	Acc \uparrow	Lat. \downarrow	Spd. \uparrow	Acc \uparrow	Lat. \downarrow	Spd. \uparrow
SLM	–	8.81	9.74	–	27.00	1.45	–	42.70	2.26	–	26.17	4.48	–
LLM-7B	–	40.90	92.46	1.00 \times	64.00	23.97	1.00 \times	78.60	38.97	1.00 \times	61.17	51.80	1.00 \times
SpecDec	–	40.31	112.21	0.82 \times	62.40	18.72	1.28 \times	80.49	47.83	0.81 \times	61.07	59.59	0.87 \times
R-Stitch	0.001	40.31	87.67	1.05 \times	59.30	19.62	1.22 \times	74.40	22.32	1.75 \times	58.00	43.20	1.20 \times
R-Stitch	0.005	41.88	82.12	1.07 \times	48.90	13.65	1.76 \times	67.70	14.18	2.75 \times	52.83	36.65	1.41 \times
R-Stitch	0.01	36.59	78.54	1.18 \times	49.70	10.98	2.18 \times	62.80	7.46	5.22 \times	49.70	32.33	1.60 \times
LLM-14B	–	49.51	183.26	1.00 \times	74.90	7.52	1.00 \times	86.00	25.10	1.00 \times	70.14	71.96	1.00 \times
SpecDec	–	42.27	234.62	0.78 \times	72.20	4.25	1.77 \times	78.60	16.92	1.48 \times	64.36	85.26	0.84 \times
R-Stitch	0.001	40.90	160.10	1.14 \times	68.85	7.13	1.06 \times	77.40	16.65	1.51 \times	62.38	61.29	1.17 \times
R-Stitch	0.005	36.20	142.03	1.29 \times	62.40	5.83	1.29 \times	70.10	8.06	3.11 \times	56.23	51.97	1.38 \times
R-Stitch	0.01	37.78	131.43	1.39 \times	56.10	4.30	1.75 \times	73.20	5.86	4.28 \times	55.69	47.20	1.52 \times

benchmarks. Nevertheless, R-Stitch still enables a flexible trade-off between efficiency and accuracy across model scales. By adjusting the entropy threshold, one can smoothly interpolate between full LLM accuracy and substantially lower latency, yielding deployment options adapted to different computational budgets and latency requirements. This shows that, even when the paired SLM is less competitive, token-level hybrid decoding offers a principled and flexible mechanism to balance quality and efficiency, ensuring that practitioners can extract most of the benefits of large models at significantly reduced cost.

A.7. Comparison with Same-Family Speculative Decoding

We report results where speculative decoding is evaluated using both the model pairs in the manuscript and the same-family DeepSeek-R1-Distill-Qwen draft-target pairs with higher consistency (marked with *). All results in Table 6 show accuracy (%) and latency (s) under an 8k budget. We highlight in **bold** the best acceleration achieved without any accuracy drop. While same-family pairing improves speculative decoding by increasing draft-target agreement, its acceleration remains limited because strict token-level consistency is still required. R-Stitch achieves comparable or better accuracy with substantially lower latency, as it does not rely on distributional alignment and can exploit concise community SLMs across model families without retraining. Extended comparisons have been added to Appendix A.9 in the revised manuscript.

Table 6. Results of speculative decoding with same-family and manuscript model pairs.

Method	AIME		AMC		MATH		Minerva	
	Acc \uparrow	Lat. \downarrow						
LLM 7B	33.33	86.63	66.27	63.15	86.00	38.34	31.62	41.79
SpecDec 7B	36.67	201.23	69.88	95.42	87.00	48.71	34.19	56.59
R-Stitch 7B	40.00	62.03	69.88	34.89	87.00	16.61	33.09	18.98
SpecDec 7B*	33.33	68.65	71.08	58.53	89.20	36.86	34.19	43.33
R-Stitch 7B*	36.67	69.73	68.67	61.16	89.20	40.55	36.76	41.15
LLM 14B	43.33	153.20	68.67	101.76	86.00	41.66	35.29	48.02
SpecDec 14B	50.00	139.10	68.67	95.59	82.80	45.88	33.46	53.02
R-Stitch 14B	43.33	87.61	69.88	41.82	85.20	20.53	35.66	22.16
SpecDec 14B*	50.00	127.59	74.70	71.39	83.80	37.02	33.46	40.95
R-Stitch 14B*	43.33	112.23	74.70	73.24	85.20	35.41	35.66	38.89

A.8. Batch Size Analysis

We report here the effect of batch size on R-Stitch latency. Because R-Stitch performs token-level switching between the SLM and LLM, the acceleration ratio naturally decreases as batch size grows; this behavior is shared by speculative-decoding-style methods, where alternating model invocations introduce synchronization points and reduce GPU utilization.

We evaluate R-Stitch and speculative decoding on the MATH dataset using the DeepSeek-R1-Distill-Qwen-7B pair within vLLM, with $\tau = 0.02$. The full LLM reaches 86.00% accuracy, and both acceleration methods obtain 87.00% accuracy. Table 7 reports average per-sample latency under each batch size. Although acceleration benefits diminish at larger batches, R-Stitch consistently achieves lower latency than speculative decoding, owing to its ability to exploit concise SLM reasoning traces beyond strict token-level consistency.

Table 7. Latency (s) of the LLM, speculative decoding, and R-Stitch across batch sizes on MATH.

Method / Batch	1	2	4	8	16	32	64	128
LLM	38.34	31.58	22.07	16.11	11.08	8.42	6.52	5.97
SpecDec	36.86	31.61	24.29	22.04	19.20	17.88	15.32	14.01
R-Stitch	16.61	20.48	17.98	14.98	12.02	10.61	7.43	6.55

A.9. Cross-Domain Evaluation

We evaluate R-Stitch ($\tau = 0.02$) and R-Stitch+ beyond mathematical reasoning on four QA and reasoning benchmarks: GPQA-D (Rein et al., 2024), ZebraLogicBench (Lin et al.), CRUXEval (Gu et al.), and MMLU-Redux (Gema et al., 2025). Accuracy (\uparrow) and latency (\downarrow) are reported. For R-Stitch+, the router is trained only on math datasets and directly applied to these domains without any retraining.

Table 8. Cross-domain evaluation on reasoning and QA benchmarks.

Method	GPQA-D		ZebraLogicBench		CRUXEval		MMLU-Redux	
	Acc \uparrow	Lat. \downarrow	Acc \uparrow	Lat. \downarrow	Acc \uparrow	Lat. \downarrow	Acc \uparrow	Lat. \downarrow
LLM-7B	23.74	171.76	21.09	91.85	70.25	14.54	74.64	20.10
SpecDec	24.24	152.23	20.22	72.03	70.50	14.78	74.04	19.37
R-Stitch	35.86	44.57	20.78	48.23	87.29	18.23	74.04	8.12
R-Stitch+	34.34	39.02	20.82	45.12	69.88	9.15	74.11	8.52

R-Stitch maintains accuracy comparable to the LLM across all tasks while providing substantial latency reductions. Moreover, R-Stitch+ consistently delivers slightly improved accuracy despite being trained only on math data, showing that its learned policy transfers well across tasks without retraining.

A.10. Architecture and Overhead of Router

The router is explicitly designed to be lightweight, and its computational and memory overhead is negligible. It is a small feed-forward network operating on SLM hidden states, composed of 6 FFN blocks with GELU and residual connections, followed by normalization and a two-head linear layer. The input matches the SLM hidden size (3584 for the 1.5B model), and the total parameter count is 0.17M. On an NVIDIA A100, the router adds 1.05 ms per invocation. At $\tau = 0.02$ on AIME with the 7B pair, it is invoked 350.38 times on average, giving 368 ms total overhead. The full inference time for the same setup is 62.03 s, so the router contributes under 0.6% of end-to-end latency, demonstrating that its deployability costs are minimal.

A.11. Computational Overhead of Entropy-Based Routing

The cost of entropy evaluation is negligible: entropy is obtained directly from the SLM logits and adds only 0.028 ms per token in our implementation. In the 7B-1.5B AIME setup ($\tau = 0.02$), decoding 4530.60 tokens takes 62.03 seconds, while entropy computation accounts for just 127 ms (approximately 0.2%), indicating no meaningful runtime burden.

A.12. Comparison with Reward-Guided Speculative Decoding

We compare R-Stitch with Reward-Guided Speculative Decoding (RSD) (Liao et al.), which performs step-level switching based on an external process reward model (PRM). Since PRMs are trained for specific target models and transfer poorly across different model pairs, RSD’s routing decisions become unstable when the draft–target model combination changes. In contrast, R-Stitch performs fine-grained token-level routing without any external supervision, providing more stable efficiency gains across diverse model pairs. Table 9 reports accuracy (%) and latency (s) under an 8k decoding budget.

Table 9. Comparison between RSD and R-Stitch under an 8k decoding budget.

Method	AIME		AMC		MATH		Minerva	
	Acc \uparrow	Lat. \downarrow						
LLM-7B	33.33	86.63	66.27	63.15	86.00	38.34	31.62	41.79
RSD-7B	30.00	69.73	66.27	54.12	81.60	25.12	33.80	54.37
R-Stitch-7B	40.00	62.03	69.88	34.89	87.00	16.61	33.09	18.98

A.13. More Per-Sample Comparisons with Speculative Decoding

Figures 6 and 7 present additional per-sample visualizations of latency speedup and token reduction when applying R-Stitch⁺ and Speculative Decoding on the LLM-7B model across more datasets beyond those reported in the main text. The supplementary results confirm the same pattern: R-Stitch⁺ consistently accelerates the majority of samples, whereas Speculative Decoding provides gains only on a minority and often leads to slowdowns due to consistency issues.

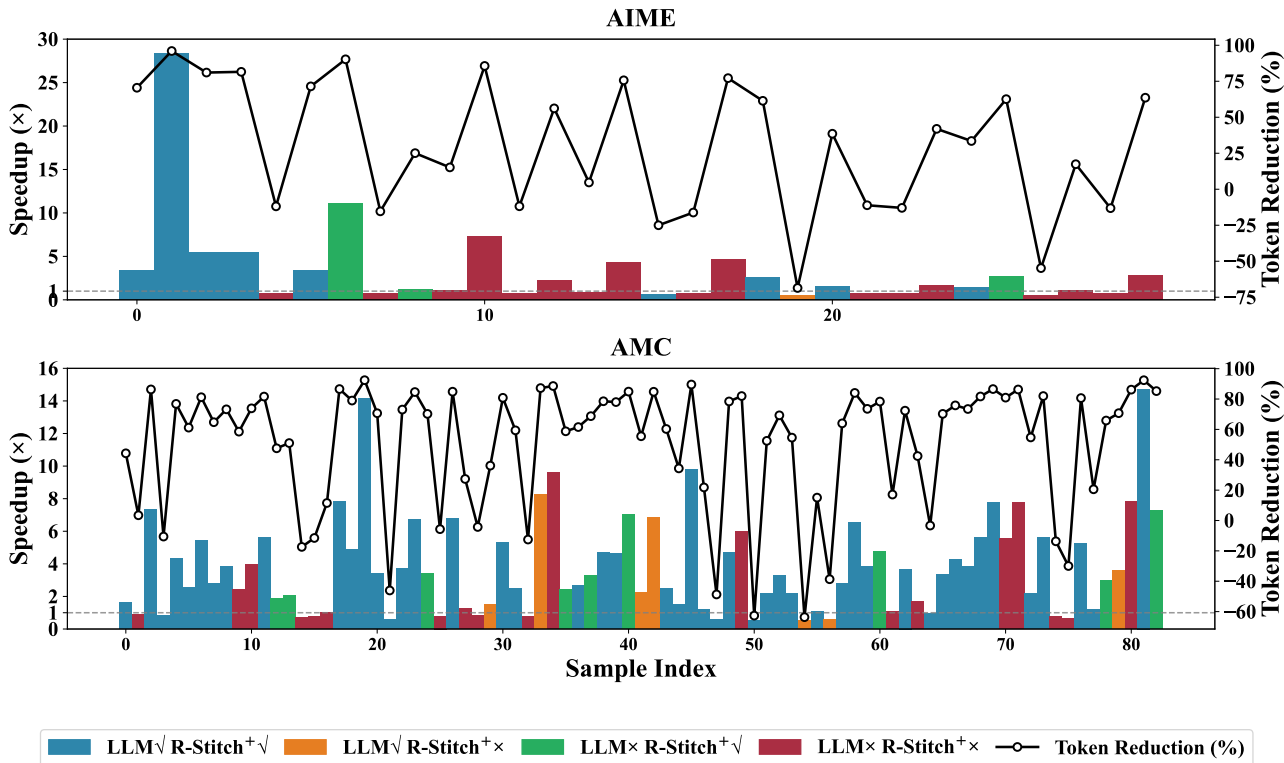


Figure 6. Per-sample visualization of R-Stitch⁺ (LLM-7B). Each bar shows the latency speedup of one sample relative to the baseline LLM. Bar colors encode correctness outcomes of the baseline and R-Stitch⁺. The dashed horizontal line at 1 indicates no speedup. The black solid curve with hollow-circle markers represents token reduction percentages per sample.

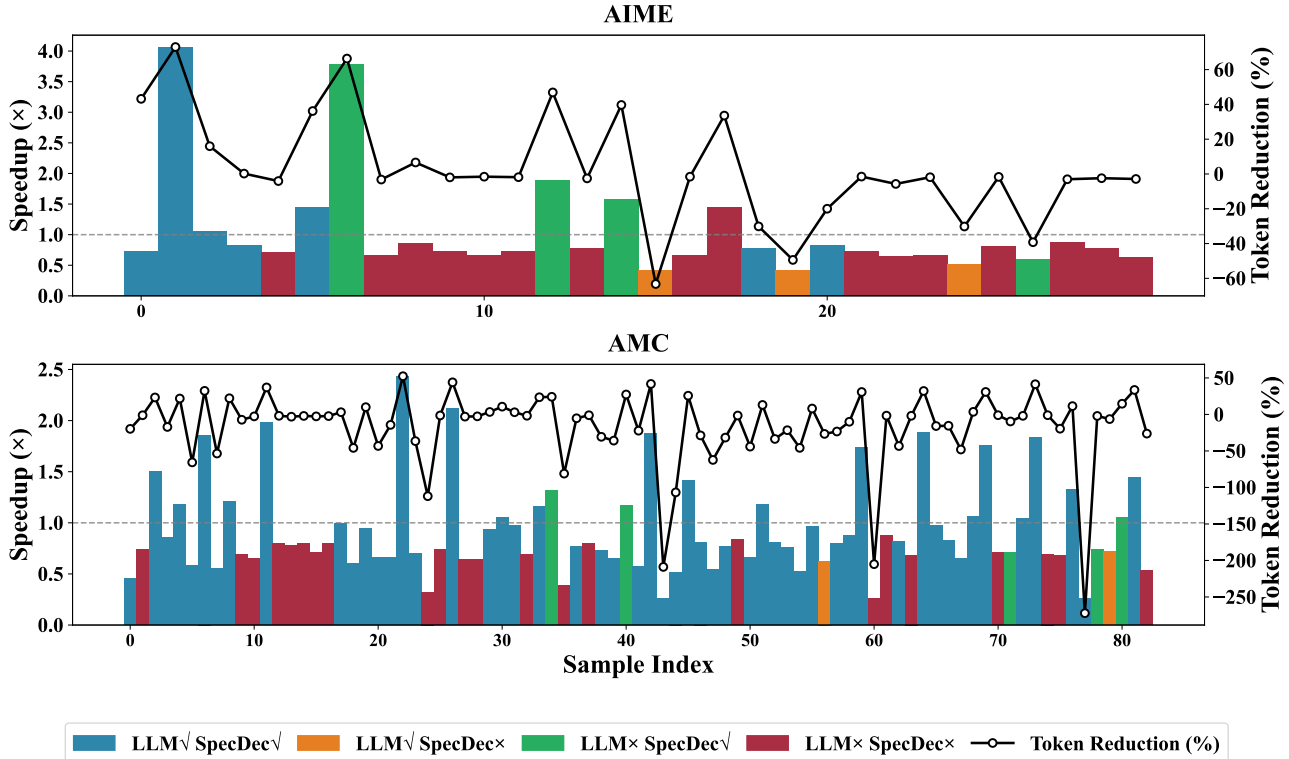


Figure 7. Per-sample visualization of Speculative Decoding (LLM-7B). Each bar shows the latency speedup of one sample relative to the baseline LLM. Bar colors encode correctness outcomes of the baseline and Speculative Decoding. The dashed horizontal line at 1 indicates no speedup. The black solid curve with hollow-circle markers represents token reduction percentages per sample.

A.14. Additional Results on Token Usage

In this section, we provide detailed tables for each dataset and benchmark under different decoding budgets as shown in Table 10 to Table 19. Beyond the main results on accuracy, latency, and relative speedup, these tables additionally report the number of tokens consumed by the LLM and the SLM, as well as the total token usage. We also compute the percentage of token reduction compared to full LLM decoding. These results offer a clearer view of how R-Stitch reduces the reliance on expensive LLM tokens across mathematical reasoning and code generation tasks, while maintaining competitive accuracy and achieving substantial efficiency improvements.

A.15. Qualitative Case Studies

To provide a more intuitive understanding of how R-Stitch leverages the complementary strengths of the SLM and LLM, we visualize several representative examples. For each selected problem, we compare the responses of the SLM, the LLM, speculative decoding, and our method R-Stitch with $\tau = 0.02$. For long outputs, we omit intermediate tokens for readability.

As shown in Figure 8 to Figure 11, the SLM alone generates very concise answers with extremely low latency but often produces incorrect solutions. The LLM eventually produces correct answers but requires thousands of tokens and much higher latency. Speculative decoding sometimes suffers from frequent token rejections under low model agreement, resulting in more decoding steps than vanilla LLM decoding and hence longer latency. In contrast, R-Stitch effectively combines the SLM’s brevity with the LLM’s accuracy: it selectively accepts confident SLM tokens while routing uncertain ones to the LLM, producing shorter but still correct solutions. This substantially reduces the number of generated tokens and yields significant acceleration.

Table 10. Comparison on **AIME** with decoding budget = 8k tokens.

Method	τ	Acc	Lat.	Spd.	LLM Tok.	SLM Tok.	Total Tok.	Reduction (%)
SLM	–	10.00	5.91	–	–	–	478.27	–
LLM-7B	–	33.33	86.63	1.00×	–	–	6699.63	–
SpecDec	–	36.67	201.23	0.43×	–	–	6922.83	+3.33%
R-Stitch	0.001	36.67	89.86	0.96×	3970.03	2916.57	6886.60	+2.79%
R-Stitch	0.02	40.00	62.03	1.40×	2607.24	1923.36	4530.60	-32.38%
R-Stitch	0.03	30.00	42.06	2.06×	1052.17	1914.37	2966.54	-55.72%
LLM-14B	–	43.33	153.20	1.00×	–	–	6243.13	–
SpecDec	–	50.00	139.10	1.10×	–	–	6192.73	-0.81%
R-Stitch	0.001	50.00	129.88	1.18×	3080.07	2498.33	5578.40	-10.65%
R-Stitch	0.02	43.33	87.61	1.75×	1693.90	2386.07	4079.97	-34.65%
R-Stitch	0.03	43.33	61.59	2.49×	1030.93	2040.03	3070.96	-50.81%
LLM-32B	–	43.33	354.85	1.00×	–	–	7334.00	–
SpecDec	–	40.00	270.25	1.31×	–	–	7540.83	+2.82%
R-Stitch	0.001	50.00	261.86	1.36×	4180.43	2613.80	6794.23	-7.36%
R-Stitch	0.02	50.00	184.97	1.92×	2486.10	3085.17	5571.27	-24.04%
R-Stitch	0.03	40.00	178.19	1.99×	2284.67	3352.27	5636.94	-23.14%

Table 11. Comparison on **AIME** with decoding budget = 16k tokens.

Method	τ	Acc	Lat.	Spd.	LLM Tok.	SLM Tok.	Total Tok.	Reduction (%)
SLM	–	10.00	5.91	–	–	–	478.27	–
LLM-7B	–	40.00	195.77	1.00×	–	–	11739.10	–
SpecDec	–	50.00	258.54	0.76×	–	–	12478.27	+6.30%
R-Stitch	0.001	46.67	192.22	1.02×	5283.83	3898.57	9182.40	-21.78%
R-Stitch	0.02	50.00	110.16	1.78×	2325.67	3402.33	5728.00	-51.21%
R-Stitch	0.03	36.67	41.51	4.72×	920.10	1753.27	2673.37	-77.23%
R-Stitch ⁺	–	50.00	86.03	2.28×	1911.24	2345.13	4256.37	-63.74%
LLM-14B	–	50.00	246.95	1.00×	–	–	9130.13	–
SpecDec	–	50.00	275.64	0.90×	–	–	6312.04	-30.87%
R-Stitch	0.001	56.67	217.06	1.14×	4476.53	3550.63	8027.16	-12.08%
R-Stitch	0.02	43.33	99.12	2.49×	1746.50	2654.30	4400.80	-51.80%
R-Stitch	0.03	40.00	54.89	4.50×	983.83	1813.63	2797.46	-69.36%
R-Stitch ⁺	–	50.00	132.98	1.86×	2784.67	2367.77	5152.44	-43.57%
LLM-32B	–	56.67	591.67	1.00×	–	–	11602.67	–
SpecDec	–	70.00	526.03	1.12×	–	–	10879.17	-6.24%
R-Stitch	0.001	70.00	488.87	1.21×	6963.43	3908.77	10872.20	-6.30%
R-Stitch	0.02	50.00	333.17	1.78×	4119.00	4431.53	8550.53	-26.31%
R-Stitch	0.03	53.33	276.03	2.14×	3302.57	4098.20	7400.77	-36.21%

Table 12. Comparison on AMC with decoding budget = 8k tokens.

Method	τ	Acc	Lat.	Spd.	LLM Tok.	SLM Tok.	Total Tok.	Reduction (%)
SLM	–	50.60	5.37	–	–	–	437.29	–
LLM-7B	–	66.27	63.15	1.00×	–	–	4796.87	–
SpecDec	–	69.88	95.42	0.66×	–	–	4922.23	+2.61%
R-Stitch	0.001	77.11	58.72	1.08×	1868.92	1792.31	3661.23	-23.67%
R-Stitch	0.02	69.88	34.89	1.81×	1365.77	1208.35	2574.12	-46.34%
R-Stitch	0.03	69.88	24.55	2.57×	484.27	1165.06	1649.33	-65.62%
R-Stitch ⁺	–	68.67	21.08	3.00×	468.72	987.24	1455.96	-69.65%
LLM-14B	–	68.67	101.76	1.00×	–	–	4199.61	–
SpecDec	–	68.67	95.59	1.06×	–	–	4495.41	+7.04%
R-Stitch	0.001	69.88	79.54	1.28×	1799.34	1803.77	3603.11	-14.20%
R-Stitch	0.02	69.88	41.82	2.43×	756.01	1366.87	2122.88	-49.45%
R-Stitch	0.03	68.67	26.43	3.85×	453.52	984.59	1438.11	-65.76%
R-Stitch ⁺	–	73.49	49.91	2.04×	1137.86	1135.87	2273.73	-45.86%
LLM-32B	–	60.24	292.78	1.00×	–	–	6081.42	–
SpecDec	–	59.04	209.72	1.40×	–	–	6102.70	+0.35%
R-Stitch	0.001	68.67	209.88	1.39×	3094.76	2131.43	5226.19	-14.06%
R-Stitch	0.02	68.67	118.26	2.48×	1567.72	2175.42	3743.14	-38.45%
R-Stitch	0.03	69.88	86.88	3.37×	1100.34	1911.72	3012.06	-50.47%

Table 13. Comparison on AMC with decoding budget = 16k tokens.

Method	τ	Acc	Lat.	Spd.	LLM Tok.	SLM Tok.	Total Tok.	Reduction (%)
SLM	–	50.60	5.37	–	–	–	437.29	–
LLM-7B	–	71.08	116.41	1.00×	–	–	7225.24	–
SpecDec	–	80.72	132.45	0.88×	–	–	9211.29	+27.49%
R-Stitch	0.001	80.72	97.26	1.20×	2902.64	2367.42	5270.06	-27.06%
R-Stitch	0.02	67.47	54.17	2.15×	1212.94	1830.86	3043.80	-57.87%
R-Stitch	0.03	66.27	38.07	3.06×	725.36	1505.22	2230.58	-69.13%
R-Stitch ⁺	–	77.11	56.03	2.08×	1162.74	1632.52	2795.26	-61.31%
LLM-14B	–	86.75	146.51	1.00×	–	–	5619.14	–
SpecDec	–	83.13	138.53	1.06×	–	–	4310.51	-23.29%
R-Stitch	0.001	79.52	90.72	1.61×	1968.23	1906.05	3874.28	-31.05%
R-Stitch	0.02	66.27	51.29	2.86×	900.52	1524.18	2424.70	-56.85%
R-Stitch	0.03	63.86	28.38	5.16×	460.84	1062.13	1522.97	-72.90%
R-Stitch ⁺	–	78.31	68.50	2.14×	1476.96	1450.69	2927.65	-47.90%
LLM-32B	–	87.95	419.94	1.00×	–	–	8384.20	–
SpecDec	–	87.95	326.73	1.29×	–	–	8217.63	-1.99%
R-Stitch	0.001	90.36	288.92	1.45×	4251.51	2716.18	6967.69	-16.89%
R-Stitch	0.02	81.93	168.19	2.50×	2081.64	2629.07	4710.71	-43.81%
R-Stitch	0.03	73.49	143.53	2.93×	1639.04	2661.71	4300.75	-48.70%

Table 14. Comparison on **Minerva** with decoding budget = 8k tokens.

Method	τ	Acc	Lat.	Spd.	LLM Tok.	SLM Tok.	Total Tok.	Reduction (%)
SLM	–	25.37	5.03	–	–	–	408.08	–
LLM-7B	–	31.62	41.79	1.00×	–	–	2966.47	–
SpecDec	–	34.19	56.59	0.74×	–	–	3293.91	+11.04%
R-Stitch	0.001	34.19	38.73	1.08×	1320.15	1141.49	2461.64	-17.02%
R-Stitch	0.02	33.09	18.98	2.20×	455.23	820.51	1275.74	-56.99%
R-Stitch	0.03	33.09	17.72	2.36×	375.65	803.61	1179.26	-60.25%
R-Stitch ⁺	–	35.29	15.33	2.73×	398.68	756.12	1154.80	-61.07%
LLM-14B	–	35.29	48.02	1.00×	–	–	3348.93	–
SpecDec	–	34.93	53.02	0.91×	–	–	3216.78	-3.95%
R-Stitch	0.001	35.66	40.54	1.18×	1014.94	925.07	1940.01	-42.07%
R-Stitch	0.02	35.66	22.16	2.17×	409.41	776.69	1186.10	-64.58%
R-Stitch	0.03	34.93	17.59	2.73×	299.85	674.68	974.53	-70.90%
R-Stitch ⁺	–	35.66	26.66	1.80×	775.71	763.89	1539.60	-54.03%
LLM-32B	–	41.18	231.10	1.00×	–	–	4720.20	–
SpecDec	–	41.91	182.28	1.27×	–	–	4724.27	+0.09%
R-Stitch	0.001	42.65	141.24	1.64×	2309.25	1529.28	3838.53	-18.68%
R-Stitch	0.02	36.76	59.58	3.88×	831.41	1176.50	2007.91	-57.46%
R-Stitch	0.03	34.56	43.41	5.32×	578.15	1002.49	1580.64	-66.51%

Table 15. Comparison on **Minerva** with decoding budget = 16k tokens.

Method	τ	Acc	Lat.	Spd.	LLM Tok.	SLM Tok.	Total Tok.	Reduction (%)
SLM	–	25.37	5.03	–	–	–	408.08	–
LLM-7B	–	34.93	54.43	1.00×	–	–	3616.44	–
SpecDec	–	35.66	115.76	0.47×	–	–	5987.29	+65.56%
R-Stitch	0.001	35.66	45.53	1.20×	1482.54	1272.18	2754.72	-23.83%
R-Stitch	0.02	33.09	18.79	2.90×	443.68	810.42	1254.10	-65.32%
R-Stitch	0.03	35.29	13.50	4.03×	295.17	663.07	958.24	-73.50%
R-Stitch ⁺	–	35.29	13.68	3.98×	283.08	667.68	950.76	-73.71%
LLM-14B	–	39.34	68.99	1.00×	–	–	2801.30	–
SpecDec	–	39.34	55.40	1.25×	–	–	3521.18	+25.70%
R-Stitch	0.001	37.87	40.46	1.71×	990.31	924.97	1915.28	-31.63%
R-Stitch	0.02	31.99	22.74	3.03×	416.56	784.71	1201.27	-57.12%
R-Stitch	0.03	33.82	16.14	4.27×	263.77	645.72	909.49	-67.53%
R-Stitch ⁺	–	37.13	35.11	1.96×	810.15	810.38	1620.53	-42.15%
LLM-32B	–	46.69	348.48	1.00×	–	–	5553.52	–
SpecDec	–	44.23	273.07	1.28×	–	–	5982.18	+7.72%
R-Stitch	0.001	41.18	126.62	2.75×	2013.80	1605.40	3619.20	-34.83%
R-Stitch	0.02	40.07	73.32	4.75×	900.55	1923.00	2823.55	-49.16%
R-Stitch	0.03	36.40	43.58	8.00×	302.19	626.28	928.47	-83.28%

Table 16. Comparison on **MATH** with decoding budget = 8k tokens.

Method	τ	Acc	Lat.	Spd.	LLM Tok.	SLM Tok.	Total Tok.	Reduction (%)
SLM	–	73.60	4.56	–	–	–	370.67	–
LLM-7B	–	86.00	38.34	1.00×	–	–	2753.01	–
SpecDec	–	87.00	48.71	0.79×	–	–	3048.78	+10.74%
R-Stitch	0.001	89.40	32.94	1.16×	1022.38	1101.67	2124.05	-22.85%
R-Stitch	0.02	87.00	16.61	2.31×	344.28	770.52	1114.80	-59.51%
R-Stitch	0.03	85.60	15.15	2.53×	280.26	748.21	1028.47	-62.64%
R-Stitch ⁺	–	86.60	15.68	2.45×	503.17	598.88	1102.05	-59.97%
LLM-14B	–	86.00	41.66	1.00×	–	–	2934.52	–
SpecDec	–	82.80	45.88	0.91×	–	–	2443.78	-16.72%
R-Stitch	0.001	89.00	37.03	1.13×	867.72	937.65	1805.37	-38.48%
R-Stitch	0.02	85.20	20.53	2.03×	349.82	749.75	1099.57	-62.53%
R-Stitch	0.03	83.40	14.77	2.82×	215.10	645.26	860.36	-70.68%
R-Stitch ⁺	–	88.20	29.08	1.43×	635.27	764.58	1399.85	-52.30%
LLM-32B	–	87.20	178.38	1.00×	–	–	3054.16	–
SpecDec	–	88.60	136.73	1.30×	–	–	3052.70	-0.05%
R-Stitch	0.001	91.20	95.49	1.87×	1507.99	1322.78	2830.77	-7.31%
R-Stitch	0.02	90.60	80.21	2.22×	1087.60	1209.95	2297.55	-24.77%
R-Stitch	0.03	87.00	32.21	5.54×	387.09	890.72	1277.81	-58.16%

Table 17. Comparison on **MATH** with decoding budget = 16k tokens.

Method	τ	Acc	Lat.	Spd.	LLM Tok.	SLM Tok.	Total Tok.	Reduction (%)
SLM	–	73.60	4.56	–	–	–	370.67	–
LLM-7B	–	90.80	50.07	1.00×	–	–	3381.51	–
SpecDec	–	91.20	44.47	1.13×	–	–	2645.27	-21.77%
R-Stitch	0.001	91.00	38.34	1.31×	1136.11	1151.15	2287.26	-32.36%
R-Stitch	0.02	88.60	22.56	2.22×	451.49	908.54	1360.03	-59.78%
R-Stitch	0.03	83.20	15.62	3.21×	275.91	729.55	1005.46	-70.27%
R-Stitch ⁺	–	88.60	16.02	3.13×	278.17	732.16	1010.33	-70.12%
LLM-14B	–	88.60	66.54	1.00×	–	–	2698.10	–
SpecDec	–	87.40	67.18	0.99×	–	–	2681.58	-0.61%
R-Stitch	0.001	89.40	39.82	1.67×	886.11	958.29	1844.40	-31.64%
R-Stitch	0.02	87.80	22.62	2.94×	365.23	793.84	1159.07	-57.04%
R-Stitch	0.03	84.80	17.37	3.83×	237.71	687.69	925.40	-65.70%
R-Stitch ⁺	–	89.60	33.70	1.97×	719.47	811.61	1531.08	-43.25%
LLM-32B	–	94.00	249.92	1.00×	–	–	4304.52	–
SpecDec	–	93.20	187.79	1.33×	–	–	4023.25	-6.53%
R-Stitch	0.001	94.00	172.08	1.45×	952.53	905.83	1858.36	-56.83%
R-Stitch	0.02	90.60	80.21	3.12×	1087.60	1209.95	2297.55	-46.62%
R-Stitch	0.03	87.80	38.32	6.52×	148.40	467.67	616.07	-85.69%

Table 18. Comparison on **OlympiadBench** with decoding budget = 8k tokens.

Method	τ	Acc	Lat.	Spd.	LLM Tok.	SLM Tok.	Total Tok.	Reduction (%)
SLM	–	36.89	5.42	–	–	–	441.54	–
LLM-7B	–	51.85	117.31	1.00×	–	–	5109.47	–
SpecDec	–	51.85	134.23	0.87×	–	–	5292.34	+3.58%
R-Stitch	0.001	55.26	105.29	1.11×	1551.23	1216.72	2767.95	-45.83%
R-Stitch	0.02	51.85	70.43	1.67×	487.93	810.37	1298.30	-74.59%
R-Stitch	0.03	48.59	51.43	2.28×	280.62	647.15	927.77	-81.84%
R-Stitch ⁺	–	52.00	45.02	2.61×	374.52	679.23	1053.75	-79.38%
LLM-14B	–	54.07	190.89	1.00×	–	–	4623.48	–
SpecDec	–	54.22	180.03	1.06×	–	–	5320.88	+15.08%
R-Stitch	0.001	54.22	165.07	1.16×	1285.81	938.74	2224.55	-51.89%
R-Stitch	0.02	52.44	96.09	1.99×	375.46	668.54	1044.00	-77.42%
R-Stitch	0.03	48.44	52.36	3.65×	214.74	556.72	771.46	-83.31%
R-Stitch ⁺	–	56.30	108.67	1.76×	906.33	809.67	1716.00	-62.89%
LLM-32B	–	50.67	379.52	1.00×	–	–	5988.08	–
SpecDec	–	50.37	351.27	1.08×	–	–	4564.46	-23.77%
R-Stitch	0.001	50.67	341.67	1.11×	2441.57	1432.92	3874.49	-35.30%
R-Stitch	0.02	53.78	226.71	1.67×	488.88	781.20	1270.08	-78.79%
R-Stitch	0.03	52.15	157.47	2.41×	515.87	968.86	1484.73	-75.21%

Table 19. Comparison on **OlympiadBench** with decoding budget = 16k tokens.

Method	τ	Acc	Lat.	Spd.	LLM Tok.	SLM Tok.	Total Tok.	Reduction (%)
SLM	–	36.89	5.42	–	–	–	441.54	–
LLM-7B	–	58.67	208.77	1.00×	–	–	6839.96	–
SpecDec	–	60.15	267.03	0.78×	–	–	7208.65	+5.39%
R-Stitch	0.001	60.15	201.13	1.04×	1817.81	1327.43	3145.24	-54.02%
R-Stitch	0.02	58.67	109.98	1.90×	504.00	840.55	1344.55	-80.34%
R-Stitch	0.03	54.22	65.65	3.18×	288.84	664.50	953.34	-86.06%
R-Stitch ⁺	–	59.11	95.31	2.19×	498.17	814.36	1312.53	-80.81%
LLM-14B	–	60.00	316.06	1.00×	–	–	6024.14	–
SpecDec	–	60.00	360.14	0.88×	–	–	6143.46	+1.98%
R-Stitch	0.001	61.04	69.28	4.56×	1516.14	1225.07	2741.21	-54.50%
R-Stitch	0.02	54.22	108.61	2.91×	449.36	771.67	1221.03	-79.73%
R-Stitch	0.03	48.59	68.63	4.61×	257.66	623.88	881.54	-85.37%
R-Stitch ⁺	–	59.11	121.39	2.60×	982.06	846.84	1828.90	-69.64%
LLM-32B	–	67.70	722.77	1.00×	–	–	8524.71	–
SpecDec	–	67.70	798.23	0.91×	–	–	7495.21	-12.08%
R-Stitch	0.001	66.07	654.24	1.10×	6415.09	2689.76	9104.85	+6.81%
R-Stitch	0.02	61.12	358.87	2.01×	3779.95	2954.05	6734.00	-21.01%
R-Stitch	0.03	55.70	209.96	3.44×	625.54	1085.62	1711.16	-79.93%

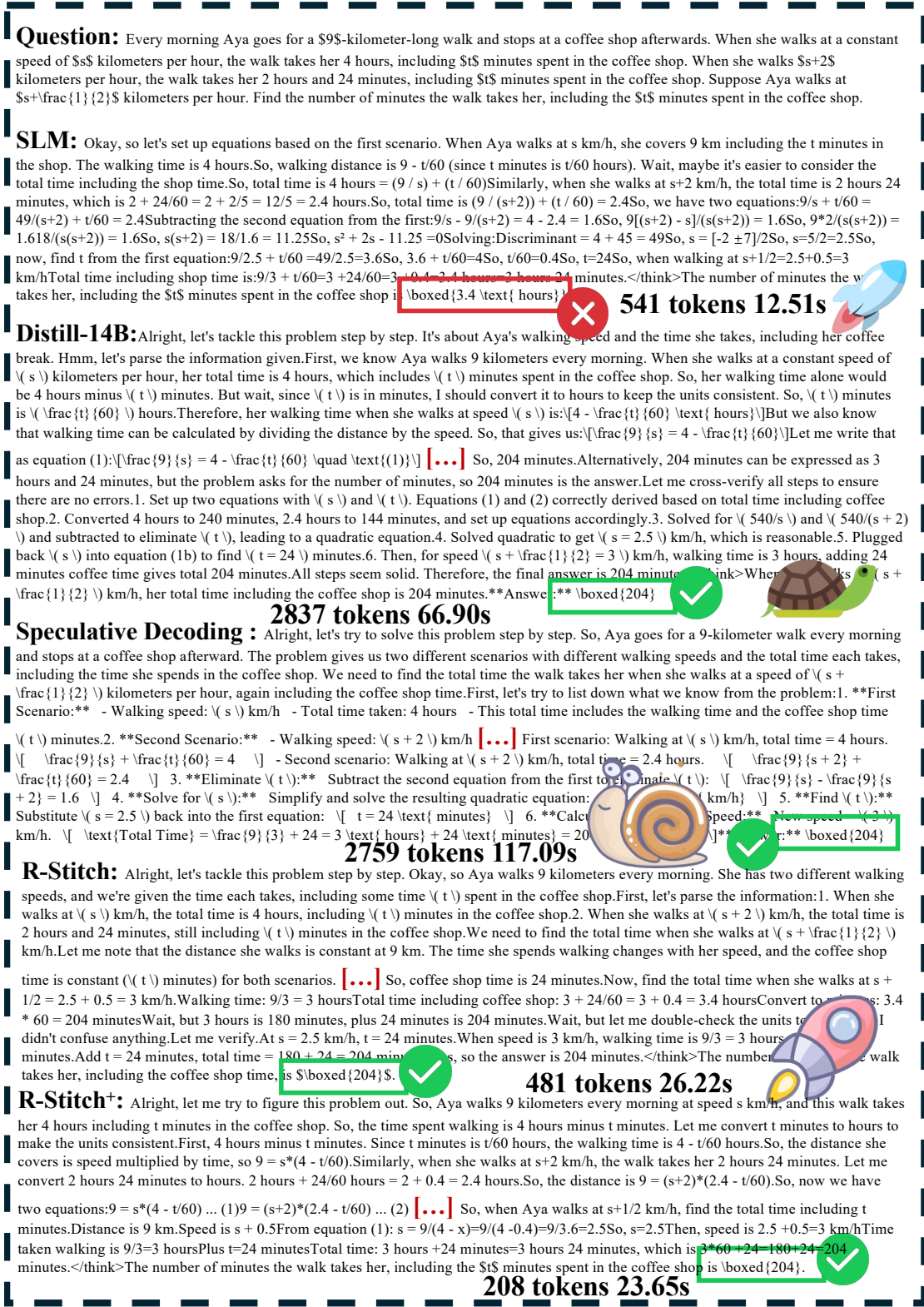
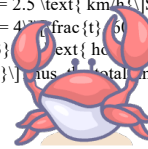


Figure 8. Qualitative comparison of outputs. Each case shows the predicted solution, token count, and latency for the SLM, LLM, speculative decoding, and R-Stitch ($\tau = 0.02$). R-Stitch produces concise and correct reasoning while reducing token count and latency compared to LLM decoding.

Question: Every morning Aya goes for a 9-kilometer-long walk and stops at a coffee shop afterwards. When she walks at a constant speed of s kilometers per hour, the walk takes her 4 hours, including t minutes spent in the coffee shop. When she walks $s+2$ kilometers per hour, the walk takes her 2 hours and 24 minutes, including t minutes spent in the coffee shop. Suppose Aya walks at $s+\frac{1}{2}$ kilometers per hour. Find the number of minutes the walk takes her, including the t minutes spent in the coffee shop.

SLM: Okay, so let's set up equations based on the first scenario. When Aya walks at s km/h, she covers 9 km including the t minutes in the shop. The walking time is 4 hours. So, walking distance is $9 - t/60$ (since t minutes is $t/60$ hours). Wait, maybe it's easier to consider the total time including the shop time. So, total time is 4 hours = $(9/s) + (t/60)$. Similarly, when she walks at $s+2$ km/h, the total time is 2 hours 24 minutes, which is $2 + 24/60 = 2 + 2/5 = 12/5 = 2.4$ hours. So, total time is $(9/(s+2)) + (t/60) = 2.4$. So, we have two equations: $9/s + t/60 = 4$ and $9/(s+2) + t/60 = 2.4$. Subtracting the second equation from the first: $9/s - 9/(s+2) = 4 - 2.4 = 1.6$. So, $9[(s+2) - s]/(s(s+2)) = 1.6$. $9*2/(s(s+2)) = 1.6$. So, $s(s+2) = 18/1.6 = 11.25$. So, $s^2 + 2s - 11.25 = 0$. Solving: Discriminant = $4 + 45 = 49$. So, $s = [-2 \pm 7]/2$. So, $s = 5/2 = 2.5$. So, now, find t from the first equation: $9/2.5 + t/60 = 4$. $3.6 + t/60 = 4$. $t/60 = 0.4$. $t = 24$. So, when walking at $s+1/2 = 2.5 + 0.5 = 3$ km/h, total time including shop time is: $9/3 + t/60 = 3 + 24/60 = 3 + 0.4 = 3.4$ hours = 2 hours 24 minutes. The number of minutes the walk takes her, including the t minutes spent in the coffee shop is $\boxed{3.4 \text{ hours}}$.  **541 tokens 12.51s** 

QWQ-32B: Okay, so I need to solve this problem about Aya's walk and coffee shop stop. Let me try to parse the information step by step. First, the problem says that every morning Aya goes for a 9-kilometer walk and then stops at a coffee shop. The key points here are that the walk is 9 km long, and she spends some time t minutes at the coffee shop. The problem gives two scenarios with different walking speeds and total times, and then asks for the total time when she walks at a different speed. Let me note down the given data: 1. **First scenario:** - Walking speed: s km/h - Total time taken (including t minutes in coffee shop): 4 hours - Distance: 9 km. 2. **Second scenario:** - Walking speed: $s + 2$ km/h - Total time taken (including same t minutes): 2 hours and 24 minutes - Distance: 9 km. ****Question:**** - Find total time (in minutes) when walking at $s + 0.5$ km/h, including t minutes. **[...]** Subtracting the second equation from the first to eliminate the term involving t : $9/s - 9/(s+2) = 4 - 2.4 = 1.6$. Converting to a common denominator and simplifying: $9(s+2) - 9s = 1.6s(s+2)$. $18 = 1.6s^2 + 3.2s$. $180 = 16s^2 + 32s$. $16s^2 + 32s - 180 = 0$. Dividing by 4: $4s^2 + 8s - 45 = 0$. Using the quadratic formula: $s = \frac{-8 \pm \sqrt{64 + 720}}{8} = \frac{-8 \pm \sqrt{784}}{8} = \frac{-8 \pm 28}{8}$. Discarding negative solution because speed is positive: $s = (20)/8 = 2.5$ km/h. Substituting $s = 2.5$ back into the first equation to find t : $9/2.5 + t/60 = 4$. $3.6 + t/60 = 4$. $t/60 = 0.4$. $t = 24$ minutes. For the new speed $s + 0.5 = 3$ km/h, the walking time is $9/3 = 3$ hours. Adding the coffee shop time $t = 24$ minutes, the total time is $3 \text{ hours} + 24 \text{ minutes} = 3 \text{ hours } 24 \text{ minutes}$. Thus, the number of minutes the walk takes her, including the t minutes spent in the coffee shop, is $\boxed{204}$.  **4631 tokens 172.95s** 

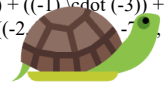
Speculative Decoding : Okay, so I need to solve this problem about Aya's walk and coffee shop stop. Let me read it again and try to understand what's going on. Every morning, Aya goes for a 9-kilometer walk and then stops at a coffee shop. The problem gives two different scenarios where she walks at different speeds, and each time the total time (including the coffee shop stop) is different. The question is asking, if she walks at $s + 1/2$ km/h, how many minutes will the whole thing take, including the t minutes in the coffee shop. First, let's parse the information given. There are two scenarios: 1. When she walks at speed s km/h, the total time (walking + coffee) is 4 hours, which is 240 minutes. The time spent in the coffee shop is t minutes, so the walking time must be $(240 - t)$ minutes. 2. When she walks at speed $(s + 2)$ km/h, the total time is 2 hours and 24 minutes. Converting that to minutes, 2 hours is 120 minutes, plus 24 minutes is 144 minutes. Again, the coffee shop time is t minutes, so the walking time here is $(144 - t)$ minutes. **[...]** Subtracting the second equation from the first to eliminate t : $9/s - 9/(s+2) = 4 - 2.4 = 1.6$. Simplifying: $9(s+2) - 9s = 1.6s(s+2)$. $18 = 1.6s^2 + 3.2s$. $180 = 16s^2 + 32s$. $16s^2 + 32s - 180 = 0$. Dividing by 4: $4s^2 + 8s - 45 = 0$. Using the quadratic formula: $s = \frac{-8 \pm \sqrt{64 + 720}}{8} = \frac{-8 \pm \sqrt{784}}{8} = \frac{-8 \pm 28}{8}$. Discarding negative solution because speed is positive: $s = (20)/8 = 2.5$ km/h. Substituting $s = 2.5$ back into the first equation to find t : $9/2.5 + t/60 = 4$. $3.6 + t/60 = 4$. $t/60 = 0.4$. $t = 24$ minutes. When walking at $s + 1/2 = 3$ km/h, the walking time is $9/3 = 3$ hours = 180 minutes. Adding the coffee shop time $t = 24$ minutes: $180 + 24 = 204$ minutes. Thus, the total time Aya takes when walking at $(s + 1/2)$ km/h is $\boxed{204}$.  **3128 tokens 123.21s** 

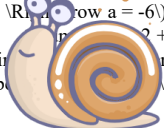
R-Stitch: Let's see. So, Aya walks 9 kilometers at speed s km/h, takes her 4 hours including t minutes in the coffee shop. When she walks at $s+2$ km/h, it takes her 2 hours 24 minutes (which is 2.4 hours) including t minutes in the coffee shop. Let's set up equations. Time spent walking plus coffee time equals total time. First, the time to walk 9 km at speed s is $9/s$ hours. This includes t minutes in the coffee shop, so: $9/s = (\text{total time} - t \text{ minutes in hours})$. Wait, actually, wait. Wait, total time is the time walking plus time at coffee shop. Wait, the problem says the walk takes her 4 hours including t minutes spent in the coffee shop. So, the walk itself (the walking time) plus t minutes is the total time. So, walking time = 4 hours - t minutes. Wait, but units might be inconsistent. Let me make sure. Alternatively: Let me denote the time she spends walking as T_1 and T_2 , and the time at the coffee shop is fixed as t minutes regardless of speed. So, when she walks at s km/h, the walking time is $9/s$, and the total time is 4 hours. So, $9/s + t/60 = 4$. Similarly, when she walks at $s+2$ km/h, the walking time is $9/(s+2)$, and the total time is 2h24m = $2 + 24/60 = 2 + 0.4 = 2.4$ hours. So, $9/(s+2) + t/60 = 2.4$. So, equations: $9/s + t/60 = 4$... (1) $9/(s+2) + t/60 = 2.4$... (2) Subtract (2) from (1): $9/s - 9/(s+2) = 4 - 2.4 = 1.6$. Simplify: $9((s+2) - s)/(s(s+2)) = 1.6$. $9(2)/(s(s+2)) = 1.6$. $18/(s(s+2)) = 1.6$. $18 = 1.6s(s+2)$. $180 = 16s^2 + 32s$. $16s^2 + 32s - 180 = 0$. Divide by 4: $4s^2 + 8s - 45 = 0$. Use quadratic formula: $s = \frac{-8 \pm \sqrt{64 + 720}}{8} = \frac{-8 \pm \sqrt{784}}{8} = \frac{-8 \pm 28}{8}$. Discarding negative solution because speed is positive: $s = (20)/8 = 2.5$. Wait, that's $s = 2.5$ km/h. Then, find t from equation (1): $9/2.5 + t/60 = 4$. $3.6 + t/60 = 4$. $t/60 = 0.4$. $t = 24$ minutes. Let me find the second equation as check: $9/(2.5+2) + 24/60 = 9/4.5 + 0.4 = 2 + 0.4 = 2.4$, which is correct. So, the problem asks for the total time when walking at $s + 1/2 = 2.5 + 0.5 = 3$ km/h, how much time does the walk take? The total time is $9/3 + t/60 = 3 + 0.4 = 3.4$ hours = 2 hours 24 minutes. Converting to minutes including t : $3 \text{ hours} + 24 \text{ minutes} = 204$ minutes. The number of minutes the walk takes including the t minutes spent in the coffee shop is $\boxed{204}$.  **652 tokens 20.25s** 

Figure 9. Qualitative comparison of outputs. Each case shows the predicted solution, token count, and latency for the SLM, LLM, speculative decoding, and R-Stitch ($\tau = 0.02$). R-Stitch produces concise and correct reasoning while reducing token count and latency compared to LLM decoding.

Question: For how many ordered pairs (a,b) of integers does the polynomial $Sx^3+ax^2+bx+6S$ have $3S$ distinct integer roots?

SLM: Okay, so we need to find integer pairs (a,b) such that the polynomial $x^3 + ax^2 + bx + 6$ has three distinct integer roots. Let's call the roots $r, s,$ and t . So, by Vieta's formulas: $r + s + t = -a$, $rs + rt + st = -b$, $rst = 6$. So, we need to find triples of integers r, s, t such that their product is -6 . Let's list all possible triples. The factors of 6 are $\pm 1, \pm 2, \pm 3, \pm 6$. So, possible triples: $(1, 2, -3), (-1, -2, 3), (1, -1, 6), (-1, 1, -6), (2, -1, -3), (-2, 1, 3), (3, -1, -2), (-3, 1, 2), (6, -1, -1), (-6, 1, 1)$. Wait, let's find all triplets of integers whose product is -6 . Possible triplets: $(1, 1, -6), (1, -1, 6), (2, -1, 3), (-2, 1, 3), (3, -1, -2), (-3, 1, 2), (6, -1, -1), (-6, 1, 1)$. But they need to be distinct integers, so we eliminate triplets with repeated elements. So, possible triplets: $(1, 2, -3), (-1, -2, 3), (1, -1, 6), (-1, 1, -6), (2, -1, -3), (-2, 1, 3), (3, -1, -2), (-3, 1, 2), (6, -1, -1), (-6, 1, 1)$. So, let's consider each triplet. Case 1: Roots $1, 2, -3$. Then, sum: $1 + 2 + (-3) = 0 = -a \Rightarrow a = 0$. Sum of products: $(1)(2) + (1)(-3) + (2)(-3) = 2 - 3 - 6 = -7 = -b \Rightarrow b = 7$. So, this triplet gives $a=0, b=7$. Case 2: Roots $1, -1, 6$. Sum: $1 + (-1) + 6 = 6 = -a \Rightarrow a = -6$. Sum of products: $(1)(-1) + (1)(6) + (-1)(6) = -1 + 6 - 6 = -1 = -b \Rightarrow b = 1$. So, this triplet gives $a=-6, b=1$. Case 3: Roots $-1, 2, -3$. Sum: $-1 + 2 + (-3) = -2 = -a \Rightarrow a = 2$. Sum of products: $(-1)(2) + (-1)(-3) + (2)(-3) = -2 + 3 - 6 = -5 = -b \Rightarrow b = 5$. So, this triplet gives $a=2, b=5$. So, total triplets are three pairs: $(0, 7), (-6, 1), (2, 5)$. So, the number of ordered pairs (a, b) is 3 . The number of ordered pairs (a, b) is $\boxed{3}$.  **373 tokens 5.09s** 

QWQ-32B: Okay, so I need to find the number of ordered pairs (a, b) of integers such that the polynomial $x^3 + a x^2 + b x + 6$ has three distinct integer roots. Hmm, let me think. Alright, let's start by recalling that if a polynomial has integer roots, then those roots must be divisors of the constant term when the leading coefficient is 1. Since the polynomial here is monic (leading coefficient 1), the roots must be integers that multiply to 6 (because the constant term is 6 , right? By Vieta's formula). So, first, maybe I should list all the possible integer divisors of 6 and find all triplets of distinct integers that multiply to 6 . Each triplet will correspond to a set of roots, and from there, I can compute the coefficients a and b using Vieta's formulas, and then count the distinct ordered pairs (a, b) . Let me confirm Vieta's formulas for a cubic equation. **[...]** No valid positive roots (would require duplicate roots). **Case 2: Three negative roots:** - The triplet must be $(-1, -2, -3)$, since their product is (-6) . **Resulting Triplets:** The valid triplets are: $(-1, 1, 6)$, $(-1, 2, 3)$, $(-2, 1, 3)$, $(-3, 1, 2)$, $(-1, -2, -3)$. **Calculate (a, b) for Each Triplet:** **Triplet $(-1, 1, 6)$:** $-a = -((-1) + 1 + 6) = -6$, $-b = (-1 \cdot 1) + (-1 \cdot 6) + (1 \cdot 6) = -1 - 6 + 6 = -1$. **Pair: $(-6, -1)$.** **Triplet $(-1, 2, 3)$:** $-a = -((-1) + 2 + 3) = -4$, $-b = (-1 \cdot 2) + (-1 \cdot 3) + (2 \cdot 3) = -2 - 3 + 6 = 1$. **Pair: $(-4, 1)$.** **Triplet $(-2, 1, 3)$:** $-a = -((-2) + 1 + 3) = -2$, $-b = (-2 \cdot 1) + (-2 \cdot 3) + (1 \cdot 3) = -2 - 6 + 3 = -5$. **Pair: $(-2, -5)$.** **Triplet $(-3, 1, 2)$:** $-a = -((-3) + 1 + 2) = 0$, $-b = (-3 \cdot 1) + (-3 \cdot 2) + (1 \cdot 2) = -3 - 6 + 2 = -7$. **Pair: $(0, -7)$.** **Triplet $(-1, -2, -3)$:** $-a = -((-1) + (-2) + (-3)) = 6$, $-b = ((-1) \cdot (-2)) + ((-1) \cdot (-3)) + ((-2) \cdot (-3)) = 2 + 3 + 6 = 11$. **Pair: $(6, 11)$.** **Final Answer:** The distinct ordered pairs (a, b) are $(-6, -1), (-4, 1), (-2, -5), (0, -7), (6, 11)$. Thus, the number of such pairs is $\boxed{5}$.  **13386 tokens 683.29s** 

Speculative Decoding : Okay, so I need to find the number of ordered pairs (a, b) of integers such that the polynomial $x^3 + a x^2 + b x + 6$ has three distinct integer roots. Hmm, let me think about how to approach this. First, since the polynomial is cubic and has three distinct integer roots, I can denote those roots as $r, s,$ and t . By the Factor Theorem, the polynomial can be written as $(x - r)(x - s)(x - t)$. If I expand this, I can relate the coefficients a and b to the roots using Vieta's formulas. Let me recall Vieta's formulas for a cubic equation. For a cubic polynomial $x^3 + a x^2 + b x + c$, the sum of the roots $-a$, the sum of the products of the roots two at a time is b , and the product of the roots is $-c$. So in this case, since the polynomial is $x^3 + a x^2 + b x + 6$, we have: $r + s + t = -a$, $rs + rt + st = b$, $rst = -6$. Since we're looking for integer roots, r, s, t must be integers. Also, they must be distinct. So the problem reduces to finding all triplets of distinct integers (r, s, t) such that their product is -6 , then for each such triplet, compute a and b , and count the ordered pairs (a, b) . However, different triplets might lead to the same (a, b) , so I need to make sure I count unique pairs. **First step: find all possible triplets of integers (r, s, t) such that $r \cdot s \cdot t = -6$, and r, s, t are distinct. **[...] Step-by-Step Process:** **Identify all possible triplets** of distinct integers whose product is (-6) : **Case 1: One negative and two positive integers:** $(-1, 2, 3)$: Product $(-1 \cdot 2 \cdot 3 = -6)$, $(-2, 1, 3)$: Product $(-2 \cdot 1 \cdot 3 = -6)$, $(-3, 1, 2)$: Product $(-3 \cdot 1 \cdot 2 = -6)$, $(-1, 1, 6)$: Product $(-1 \cdot 1 \cdot 6 = -6)$. **Case 2: Three negative integers:** $(-1, -2, -3)$: Product $(-1 \cdot -2 \cdot -3 = -6)$. **Compute (a) and (b) for each triplet:** **Triplet $(-1, 2, 3)$:** $-a = -((-1) + 2 + 3) = -4$, $-b = (-1 \cdot 2) + (-1 \cdot 3) + (2 \cdot 3) = -2 - 3 + 6 = 1 \Rightarrow b = 1$. **Pair: $(-4, 1)$.** **Triplet $(-2, 1, 3)$:** $-a = -((-2) + 1 + 3) = -2$, $-b = (-2 \cdot 1) + (-2 \cdot 3) + (1 \cdot 3) = -2 - 6 + 3 = -5 \Rightarrow b = -5$. **Pair: $(-2, -5)$.** **Triplet $(-3, 1, 2)$:** $-a = -((-3) + 1 + 2) = 0$, $-b = (-3 \cdot 1) + (-3 \cdot 2) + (1 \cdot 2) = -3 - 6 + 2 = -7 \Rightarrow b = -7$. **Pair: $(0, -7)$.** **Triplet $(-1, 1, 6)$:** $-a = -((-1) + 1 + 6) = -6$, $-b = ((-1) \cdot 1) + ((-1) \cdot 6) + (1 \cdot 6) = -1 - 6 + 6 = -1 \Rightarrow b = 1$. **Pair: $(-6, -1)$.** **Triplet $(-1, -2, -3)$:** $-a = -((-1) + (-2) + (-3)) = 6$, $-b = ((-1) \cdot (-2)) + ((-1) \cdot (-3)) + ((-2) \cdot (-3)) = 2 + 3 + 6 = 11 \Rightarrow b = 11$. **Pair: $(6, 11)$.** **Verify distinct pairs:** The pairs $(-4, 1), (-2, -5), (0, -7), (-6, -1), (6, 11)$ are all distinct. Thus, the number of ordered pairs (a, b) is $\boxed{5}$.  **16347 tokens 834.41s** **

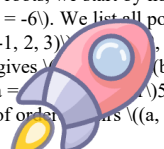
R-Stitch: To find the number of ordered pairs (a, b) of integers such that the polynomial $(x^3 + ax^2 + bx + 6)$ has 3 distinct integer roots, we can follow these steps: **Factor the Polynomial:** Since the polynomial has three distinct integer roots, it can be factored as $(x - p)(x - q)(x - r)$, where $p, q,$ and r are distinct integers. **Expand the Factored Form:** Expanding $(x - p)(x - q)(x - r)$ gives: $x^3 - (p + q + r)x^2 + (pq + pr + qr)x - pqr$. Comparing this with the given polynomial $(x^3 + ax^2 + bx + 6)$, we get: $-a = -(p + q + r)$, $b = pq + pr + qr$, $-6 = -pqr \Rightarrow pqr = 6$. **Find All Triples (p, q, r) :** We need to find all ordered triples of distinct integers (p, q, r) such that their product is -6 . **List the Integer Factorizations of -6 :** $(-1, 2, 3)$: $1 \cdot 2 \cdot (-3) = -6$, $(-1, -1, 6)$: $1 \cdot (-1) \cdot 6 = -6$, $(-1, -2, 3)$: $1 \cdot (-2) \cdot 3 = -6$, $(-2, 3, -1)$: $2 \cdot 3 \cdot (-1) = -6$, $(-1, 2, 3)$: same as above, $(-1, -3, 2)$: same as above, $(1, 3, -2)$: same as above, ... and so on. **[...] To find the number of ordered pairs (a, b) of integers such that the polynomial $(x^3 + ax^2 + bx + 6)$ has 3 distinct integer roots, we start by noting that the polynomial can be factored as $(x - p)(x - q)(x - r)$ where (p, q, r) are distinct integers. The product $(pqr = -6)$. We list all possible triplets of distinct integers whose product is -6 . These triplets are: $(1, 2, -3)$, $(1, -1, 6)$, $(1, -2, 3)$, $(-1, -2, 3)$, $(-1, 1, 6)$, $(-2, 1, 3)$. Each triplet corresponds to a unique pair (a, b) . Calculating (a) and (b) for each triplet: $(1, 2, -3)$ gives $(a = -4, b = 1)$, $(1, -1, 6)$ gives $(a = -6, b = -1)$, $(1, -2, 3)$ gives $(a = -2, b = -5)$, $(-1, 2, 3)$ gives $(a = 0, b = -7)$, $(-1, -2, -3)$ gives $(a = 6, b = 11)$. Each of these triplets results in a unique pair (a, b) . Therefore, the number of ordered pairs (a, b) is $\boxed{5}$.  **3186 tokens 228.88s** **

Figure 10. Qualitative comparison of outputs. Each case shows the predicted solution, token count, and latency for the SLM, LLM, speculative decoding, and R-Stitch ($\tau = 0.02$). R-Stitch produces concise and correct reasoning while reducing token count and latency compared to LLM decoding.

Question: You are playing a game. A 2×1 rectangle covers two adjacent squares (oriented either horizontally or vertically) of a 3×3 grid of squares, but you are not told which two squares are covered. Your goal is to find at least one square that is covered by the rectangle. A "turn" consists of you guessing a square, after which you are told whether that square is covered by the hidden rectangle. What is the minimum number of turns you need to ensure that at least one of your guessed squares is covered by the rectangle?

SLM: Okay, so we need to find the minimum number of turns such that at least one guessed square is covered by the 2×1 rectangle on a 3×3 grid. The rectangle can be horizontal or vertical. First, let's consider the total number of squares: 9. The rectangle covers 2 squares. It can be placed in various positions: horizontally or vertically. Total number of possible positions for the rectangle: Horizontal: 3 rows, each row has 2 possible horizontal positions (columns 1-2, 2-3). So $3 \times 2 = 6$. Vertical: 3 columns, each column has 2 possible vertical positions (rows 1-2, 2-3). So $3 \times 2 = 6$. Total positions: 12. So we need to cover at least one square in each possible position with the minimum number of guesses. This is similar to a covering code problem. We need a set of squares such that every possible 2 -square rectangle covers at least one square from this set. So we need to find the smallest set of squares such that no 2 -square rectangle avoids it. In other words, the complement set should not contain any 2 -square rectangle. So we need to find the largest subset of squares that does not contain a 2 -square rectangle, and then the minimum number of guesses is $9 - \text{size of largest independent set}$. Let's find the largest subset with no 2 -square rectangle. In a 3×3 grid, a 2 -square rectangle can be horizontal or vertical. So we need to avoid having two adjacent squares in any row or column. This is similar to an independent set in a grid graph. In a 3×3 grid, the independence number is known. For a 3×3 grid, the independence number is 4. So the largest subset with no 2 -square rectangle is 4. So the minimum number of guesses is $9 - 4 = 5$. Wait, but let's confirm. In a 3×3 grid, the independence number is indeed 4. So yes, the minimum number of guesses is 5. 

454 tokens 6.28s

QWQ-32B: Okay, so I need to figure out the minimum number of turns required to guarantee that I've guessed at least one square covered by a 2×1 rectangle on a 3×3 grid. The rectangle can be placed either horizontally or vertically, and it can be anywhere on the grid. The key here is that I have to ensure that no matter where the rectangle is placed, my guesses will always hit at least one square of it. Let me think through this step by step. First, let me visualize the 3×3 grid. It has 9 squares. The rectangle can be either 2×1 or 1×2 , so it can be placed horizontally or vertically. Let me note down all possible positions where the rectangle can be placed. Starting with horizontal placements. A horizontal 2×1 rectangle occupies two adjacent squares in the same row. In a 3×3 grid, each row has 3 squares, so there are 2 possible horizontal positions per row. Since there are 3 rows, that gives $3 \times 2 = 6$ horizontal positions. Similarly, vertical placements would be

two squares in the same column. [...] The set $\{a_2, b_1, b_3, c_2\}$ is verified to intersect every possible rectangle. **Verification of the Hitting Set:** - Each rectangle is checked to ensure it includes at least one of the squares in the set: **Horizontal Rectangles:** - (a_1-a_2) : includes (a_2) - (a_2-a_3) : includes (a_2) - (b_1-b_2) : includes (b_1) - (b_2-b_3) : includes (b_3) - (c_1-c_2) : includes (c_2) - (c_2-c_3) : includes (c_2) **Vertical Rectangles:** - (a_1-b_1) : includes (b_1) - (b_1-c_1) : includes (b_1) - (a_2-b_2) : includes (a_2) - (b_2-c_2) : includes (c_2) - (a_3-b_3) : includes (b_3) - (b_3-c_3) : includes (b_3) . **Conclusion:** - The minimal hitting set requires four squares, ensuring that any possible placement of the (2×1) rectangle will include at least one of the guessed squares. - Adaptive guessing strategies can also be employed, but they do not reduce the worst-case scenario. Thus, the minimum number of turns needed is $\boxed{4}$. 

14058 tokens 723.27s

Speculative Decoding : Okay, so I need to figure out the minimum number of turns required to guarantee that at least one of my guessed squares is covered by a hidden 2×1 rectangle on a 3×3 grid. The rectangle can be placed either horizontally or vertically, covering two adjacent squares. Since it can be in different orientations and positions, I need a strategy that ensures no matter where the rectangle is, at least one of my guesses hits it. First, let me visualize the 3×3 grid. It has 9 squares, and the rectangle covers exactly two of them. The problem is asking for the minimal number of guesses required such that no matter where the rectangle is placed, at least one of my guesses is on the rectangle. I remember that in covering problems like this, the key is to minimize the maximum number of guesses that could be "missed" while still guaranteeing at least one hit. Alternatively, I need to place guesses so that every possible placement of the 2×1 rectangle includes at least one of my guessed squares. So it's kind of like a hitting set problem, where my guesses form a hitting set that intersects all possible rectangles. First, let me figure out how many possible positions the 2×1 rectangle can have. Let's see: In a 3×3 grid, horizontally placed rectangles can be in rows 1, 2, or 3, and in each row, they can be in columns 1-2 or 2-3. So that's $3 \text{ rows} \times 2 \text{ columns} = 6$ horizontal positions. [...] To determine the minimum number of turns needed to ensure that at least one guessed square is covered by a hidden 2×1 rectangle on a 3×3 grid, we need to find the smallest set of squares (hitting set) that intersects all possible placements of the rectangle. A 3×3 grid has 12 possible placements for a 2×1 rectangle (6 horizontal and 6 vertical). We need to find the smallest set of squares such that every possible rectangle includes at least one square from this set. After analyzing various configurations, we found that the following four squares form a hitting set: $(1, 2)$, $(2, 1)$, $(2, 3)$, $(3, 2)$. This set of squares ensures that every possible 2×1 rectangle (horizontal or vertical) will cover at least one of these squares. For example: - All horizontal rectangles in rows 1, 2, and 3 are covered by these squares. - All vertical rectangles in columns 1, 2, and 3 are also covered by these squares. By systematically checking all possible placements of the rectangle, we confirmed that these four squares indeed cover all 12 possible configurations. Therefore, the minimum number of turns needed to guarantee that at least one guessed square is covered is $\boxed{4}$. 

16269 tokens 809.33s

R-Stitch: To determine the minimum number of turns needed to ensure that at least one guessed square is covered by the 2×1 rectangle on a 3×3 grid, we need to analyze the problem systematically. First, the grid has 9 squares. The rectangle can be placed either horizontally or vertically, covering 2 adjacent squares. Let's count all possible positions: **Horizontal positions:** Each row has 2 possible horizontal placements (since a 2×1 rectangle covers two adjacent squares horizontally). There are 3 rows, so $3 \times 2 = 6$ horizontal positions. **Vertical positions:** [...] The pair $(3, 6)$ is $(3 \text{ and } 6)$; 6 isn't in guesses (unless guessed 3). Wait 1,5,7,9. Vertical column 2: $(2,5)$ via 5, $(5,8)$ via 5. Vertical column 3's $(3,6)$ are neither in guesses (3 and 6 are not guessed). $(6,9)$ via 9. Vertical column 1's $(1,4)$ via 1. column 1's $(4,7)$: 4 not guessed, 7 is guessed? 7 is in column 1 row 3: 7 is part of the rectangle $(1,7)$ includes 4 and 7. Since 7 is guessed, it's covered. vertical column 3 $(3,6)$ is not covered because neither 3 nor 6 are guessed. Thus $(3,6)$ is uncovered. So 1,5,7,9 misses that. Hmm. Thus 2,4,6,8 seems like a hitting set of size 4. The minimum number of turns needed is $\boxed{4}$. 

4845 tokens 328.54s

Figure 11. Qualitative comparison of outputs. Each case shows the predicted solution, token count, and latency for the SLM, LLM, speculative decoding, and R-Stitch ($\tau = 0.02$). R-Stitch produces concise and correct reasoning while reducing token count and latency compared to LLM decoding.